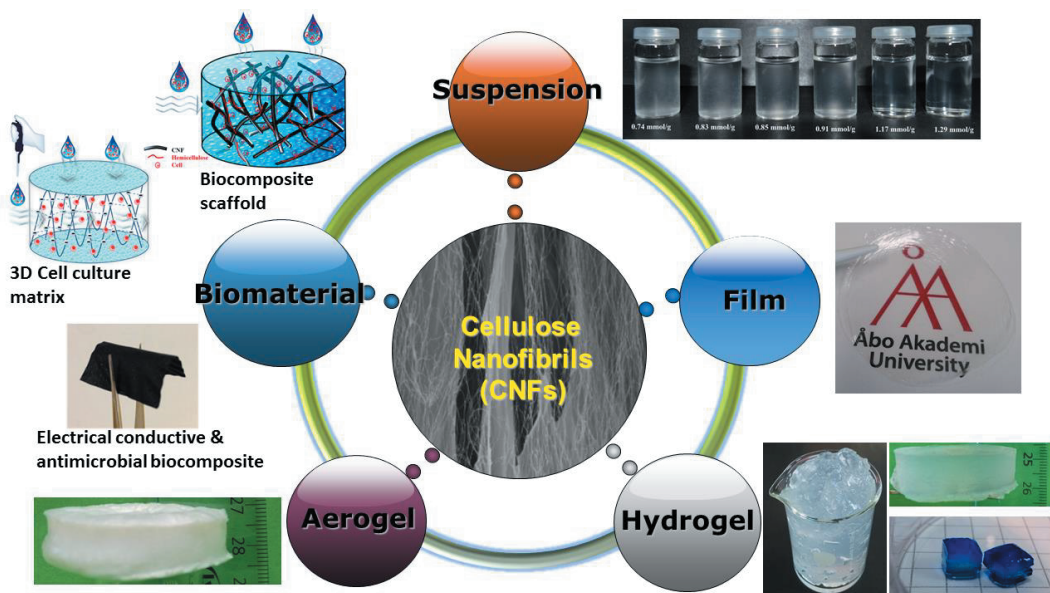


Wood-derived biomaterials for biomedical applications

Jun Liu



Laboratory of Wood and Paper Chemistry
Johan Gadolin Process Chemistry Centre
Faculty of Science and Engineering,
Åbo Akademi University
Turku/Åbo, Finland, 2016



Jun Liu

Born 1985, Mile, Yunnan, P.R. China

B.Sc. Natural Polymer Materials and Engineering: Paper-making, 2009

Tianjin University of Science and Technology, Tianjin, China

M.Sc. Pulp and Paper-making Engineering, 2012

Tianjin University of Science and Technology, Tianjin, China

Started Ph.D. research at the Laboratory of Wood and Paper Chemistry in Sept. 2012,

Åbo Akademi University, Åbo, Finland

Wood-derived biomaterials for biomedical applications

Jun Liu



Academic Dissertation

Laboratory of Wood and Paper Chemistry

Johan Gadolin Process Chemistry Centre

Faculty of Science and Engineering,

Åbo Akademi University

Turku/Åbo, Finland, 2016

Supervisors:

Docent Chunlin Xu
Laboratory of Wood and Paper Chemistry
Johan Gadolin Process Chemistry Centre
Åbo Akademi University
Åbo, Finland

Professor Stefan Willför
Laboratory of Wood and Paper Chemistry
Johan Gadolin Process Chemistry Centre
Åbo Akademi University
Åbo, Finland

Reviewers:

Professor Thomas Rosenau
Department of Chemistry
University of Nature Resources and Life Sciences
Vienna, Austria

Adjunct Professor Junyong Zhu
US Forest Service R&D
Forest Products Laboratory
University of Wisconsin-Madison
Madison, USA

Opponent:

Professor Antje Potthast
Department of Chemistry
University of Nature Resources and Life Sciences
Vienna, Austria

ISBN 978-952-12-3424-8 (Print)
ISBN 978-952-12-3425-5 (PDF)
Painosalama Oy – Turku, Finland 2016

Preface

List of publications

- I **Jun Liu**, Stefan Willför, Chunlin Xu. A review of bioactive polysaccharides: biological activities, functionalization, and biomedical applications. *Bioactive Carbohydrates and Dietary Fibre*, 2015, 5(1): 31-61.
- II **Jun Liu**, Risto Korpinen, Kirsi S. Mikkonen, Stefan Willför, Chunlin Xu. Nanofibrillated cellulose originated from birch sawdust after sequential extractions: a promising polymeric materials from waste to films. *Cellulose*, 2014, 21(4): 2587-2598.
- III Patrycja Bober, **Jun Liu**, Kirsi S. Mikkonen, Petri Ihalainen, Markus Pesonen, Carme Plumed-Ferrer, Atte von Wright, Tom Lindfors, Chunlin Xu, Rose-Marie Latonen. Biocomposites of nanofibrillated cellulose, polypyrrole and silver nanoparticles with electroconductive and antimicrobial properties. *Biomacromolecules*, 2014, 15(10): 3655-3663.
- IV **Jun Liu**, Fang Cheng, Henrik Grénman, Steven Spoljaric, Jukka Seppälä, John E. Eriksson, Stefan Willför, Chunlin Xu. Development of nanocellulose scaffolds with tunable structures to support 3D cell culture. *Carbohydrate Polymers*, 2016, 148: 259-271.
- V **Jun Liu**, Gary Chinga-Carrasco, Fang Cheng, Wenyang Xu, Stefan Willför, Kristin Syverud, Chunlin Xu. Hemicellulose-reinforced nanocellulose hydrogels for wound healing application. *Cellulose*, 2016, In press, doi: 10.1007/s10570-016-1038-3.

This work was carried out at the Laboratory of Wood and Paper Chemistry during the years of 2012-2016 under the supervision of Prof. Stefan Willför and Docent Chunlin Xu at Åbo Akademi University. Part of the work was carried out at the Wallenberg Wood Science Centre and the Division of Glycoscience, KTH Royal Institute of Technology, Sweden; and at the Paper and Fibre Research Institute (PFI) and the Department of Chemical Engineering, Norwegian University of Science and Technology, Norway.

Contribution of the author

The author of this thesis was responsible for the planning and writing of article **I**. For publication **II**, the author was responsible for the experimental works and writing of the article. In paper **III**, the author was sharing the first authorship with Patrycja Bober and

performed half of the practical experiments and writing of the manuscript. The author was responsible for planning, doing experiments and writing the articles of **IV** and **V**.

Supporting publications, proceedings, and presentations

1. **Jun Liu**, Victor Kisonen, Stefan Willför, Chunlin Xu, Francisco Vilaplana. Profiling the substitution pattern of xyloglucan derivatives by integrated enzymatic hydrolysis, hydrophilic-interaction liquid chromatography and mass spectrometry. *Journal of Chromatography A*, In press, 2016, doi:10.1016/j.chroma.2016.08.016
2. **Jun Liu**, Ann-Sofie Leppänen, Victor Kisonen, Stefan Willför, Chunlin Xu, Francisco Vilaplana. Structural analysis of galactoglucomannan and its chemical derivatives using chromatography and mass spectrometry. Manuscript, 2016.
3. Markus Peurla, Peter Kunnas, Jussi Kauppila, Antti Viinikanoja, Sauli Haataja, Rose-Marie Latonen, Patrycja Bober, Chunlin Xu, **Jun Liu**, Lauri Pelliniemi, Carita Kvarnström. Improved image contrast in low voltage transmission electron microscopy by using graphene oxide sample support. Submitted, 2016.
4. Bin Li, Wenyang Xu, Dennis Kronlund, Anni Määttänen, **Jun Liu**, Stefan Willför, Hongyan Mou, Xindong Mu, Chunlin Xu. Cellulose nanocrystals prepared via formic acid hydrolysis followed by TEMPO-mediated oxidation. *Carbohydrate Polymers*, 2015, 133: 605-612.
5. Camila Honorato, Vinay Kumar, **Jun Liu**, Hanna Koivula, Chunlin Xu, Martti Toivakka. Transparent nanocellulose-pigment composite films. *Journal of Materials Science*, 2015, 50(22): 1-10.
6. Daniel Dax, M. Soledad Chávez Bastidas, Camila Honorato, **Jun Liu**, Steven Spoljaric, Jukka Seppälä, Regis T. Mendonça, Chunlin Xu, Stefan Willför, Julio Sánchez. Tailor-made hemicellulose-based hydrogels reinforced with nanofibrillated cellulose. *Nordic Pulp and Paper Research Journal*, 2015, 30(3): 373-384.
7. Dimitar Valtakari, **Jun Liu**, Vinay Kumar, Chunlin Xu, Martti Toivakka, Jarkko J Saarinen. Conductivity of PEDOT:PSS on spin-coated and drop cast nanofibrillar cellulose thin films. *Nanoscale Research Letters*, 2015, 10: 386-396.
8. Ann-Sofie Leppänen, Chunlin Xu, **Jun Liu**, Xiaoju Wang, Markus Pesonen, Stefan Willför. Anionic polysaccharides as templates for the synthesis of conducting polyaniline and as structural matrix for conducting biocomposites. *Macromolecular Rapid Communications*, 2013, 34(13): 1056-1061.
9. Chunlin Xu, **Jun Liu**, Xiaoju Wang, Fang Cheng, Gary Chinga-Carrasco, Kristin Syverud, Stefan Willför. Nanocellulose-based scaffolds with tunable structures to support 3D cell culture. *International Conference on Nanotechnology for Renewable Materials*, proceedings abstracts, Grenoble, France, June 13th-16th, 2016.
10. Antonio Martínez-Abad, **Jun Liu**, Chunlin Xu, Francisco Vilaplana. Pattern of glycosyl and acetyl substitutions in spruce hemicelluloses using glycomic approaches. EWLP 2016, 14th European Workshop on Lignocellulosics and Pulp, Proceedings, Autrans, France, June 28th-30th, 2016

11. Antonio Martinez-Abad, Andrea C Ruthes, **Jun Liu**, Chunlin Xu, Lauren S. McKee, Vincent Bulone, Francisco Vilaplana. Glycomic approaches to unravel the intramolecular substitution pattern of hemicellulose. EPNOE 2015, the 4th EPNOE International Polysaccharide Conference, Proceeding abstracts, Warsaw, Poland, October 19th-22th, 2015.
12. Chunlin Xu, **Jun Liu**, Patrycja Bober, Tom Lindfors, Rose-Marie Latonen. Electroconductive and antimicrobial composite films of nanocellulose, polypyrrole and silver nanoparticles. ISWFPC 2015, the 18th International Symposium on Wood, Fibre and Pulping Chemistry, Proceedings, Vienna, Austria, September 9th-11th, 2015.
13. **Jun Liu**, Fang Cheng, Stefan Willför, Chunlin Xu. Nanocellulose films and aerogels with tunable structures as matrix for cellular processes in tissue engineering. EPNOE 2015, the 4th EPNOE International Polysaccharide Conference, Warsaw, Poland, October 19th-22th, 2015.
14. **Jun Liu**, Fang Cheng, Stefan Willför, Chunlin Xu. Tailoring wood cellulose to nanocomposites with controlled structure towards wound healing applications. The 8th CALSIF (Chinese Association of Life Scientists in Finland) annual meeting, Helsinki, Finland, November 29th, 2014.
15. **Jun Liu**, Chunlin Xu, Stefan Willför, Francisco Vilaplana. Structural elucidation of plant cell wall polysaccharides and their derivatives using chromatographic and mass spectrometric techniques. EWLP 2014, 13th European Workshop on Lignocellulosics and Pulp, Seville, Spain, June 24th-27th, 2014.
16. Chunlin Xu, Ann-Sofie Leppänen, **Jun Liu**, Patrycja Bober, Xiaoju Wang, Tom Lindfors, Rose-Marie Latonen, Stefan Willför. Nanofibrillated cellulose prepared from TEMPO oxidation acting as templates for synthesis of conducting polymers and in situ formation of biocomposites. EWLP 2014, the 13th European Workshop on Lignocellulosics and Pulp, Proceedings, Seville, Spain, August 24th-27th, 2014.
17. Francisco Vilaplana, **Jun Liu**, Lauren S. McKee, Chunlin Xu, Rosana Moriana, Monica EK. Glycomic tools for the structural characterization of hemicelluloses: Impact on their exploitation for novel-carbohydrate-based materials. POLYMAR 2013, International Conference in Polymers with special Focus in Early Stage Researchers, Proceeding abstracts, Crucero por el Mediteeráneo, Spain, November 8th-12th, 2013.
18. **Jun Liu**, Risto Korpinen, Kirsi S. Mikkonen, Stefan Willför, and Chunlin Xu. Nanofibrillated cellulose originated from birch sawdust after sequential extractions – a new route of developing polymeric materials in forest biorefinery. EPNOE 2013, the 3rd EPNOE International Polysaccharide Conference, Nice, France, October 21th-24th, 2013.

Contents

Preface.....	i
List of publications	i
Contribution of the author.....	i
Supporting publications, proceedings, and presentations	ii
Abstract.....	vii
Keywords	viii
Svensk sammanfattning	ix
Nyckelord.....	x
List of important abbreviations	xi
1. Introduction.....	1
1.1 Biorefinery	1
1.2 Nanocellulose.....	2
1.2.1 Cellulose nanocrystals (CNCs)	3
1.2.2 Cellulose nanofibrils (CNFs)	3
1.2.3 Bacterial cellulose (BC)	4
1.3 Hemicelluloses	4
1.4 Biocomposites.....	5
1.4.1 Nanocellulose-based biocomposites	5
1.4.2 Nanocellulose-based biomaterials for biomedical applications	5
2. Hypothesis and objectives of the work	8
3. Materials and methods	9
3.1 Materials	9
3.2 Preparation methods.....	9
3.2.1 Preparation of CNFs (Paper II, III, IV, V).....	9
3.2.2 Preparation of CNF free-standing films (Paper II, III, IV).....	10
3.2.3 Preparation of CNF polypyrrole silver composite films (CNF-PPy) (Paper III)	10
3.2.4 Preparation of CNF hydrogels and aerogels (Paper IV).....	10
3.2.5 Preparation of all-polysaccharide composite hydrogels (Paper V)	10
3.3 Biotest methods.....	11
3.3.1 Antimicrobial property of films (Paper III).....	11
3.3.2 Biocompatibility test of CNF-based scaffolds (Paper IV, V)	11
3.4 Analytical methods.....	12

3.4.1 Molar mass measurement of hemicelluloses (Paper V)	12
3.4.2 Charge density measurement of CNFs (Paper II, III, IV, V)	12
3.4.3 Transmission Electron Microscopy (TEM) imaging of CNFs (Paper II, III, IV, V)	12
3.4.4 Ultraviolet-Visible (UV-Vis) transmittance measurement of films (Paper II, V)	13
3.4.5 Fourier Transform Infrared Spectroscopy (FTIR) spectroscopy of films (Paper III, IV)	13
3.4.6 Electrical conductivity measurement of CNF-PPy composite films (Paper III)	13
3.4.7 Swelling degree measurement of films (Paper IV, V)	13
3.4.8 Topography and morphology analysis of films with laser profilometry (Paper V)	14
3.4.9 Atomic Force Microscope (AMF) imaging of films (Paper V)	14
3.4.10 Scanning Electron Microscope (SEM) imaging of aerogels (Paper IV, V)	14
3.4.11 Confocal laser scanning microscopy imaging of CNF-based scaffolds (Paper IV, V)	14
3.4.12 Tensile/compressive strength measurement of films, hydrogels, and aerogels (Paper II, III, IV, V)	15
3.4.13 Pore property analysis of aerogels (Paper IV)	15
4. Results and discussion	16
4.1 Summary and overview of the thesis work	16
4.2 Preparation of CNFs from sawdust in an integrated biorefinery process (Paper II)	16
4.2.1 Preparation and characterization of CNFs from sawdust fiber	17
4.2.2 Mechanical properties of the sawdust CNF free-standing films	21
4.3 CNF-based biocomposites with electroconductivity and antimicrobial activity (Paper III)	21
4.3.1 FTIR spectra of the CNF-PPy biocomposites	22
4.3.2 Morphology and topography of the CNF-PPy biocomposites	23
4.3.3 Mechanical, electrical conductive, and antimicrobial properties of CNF-PPy biocomposites	24
4.4 CNF-based scaffolds for 3D cell culture of tumor cells (Paper IV)	26
4.4.1 Swelling behavior of the CNF films	26
4.4.2 Porous structure and mechanical properties of the CNF scaffolds	28
4.4.3 Cell viability and proliferation in the CNF-based scaffolds	30
4.5 All-polysaccharide composite scaffolds for potential wound healing application (Paper V)	33
4.5.1 Incorporation of hemicelluloses into the CNF network and its effect on the swelling property of the composite scaffolds	34
4.5.2 Morphological properties of the all-polysaccharide composite scaffolds	36
4.5.3 Mechanical properties of the composite scaffolds	37
4.5.4 CNF composite scaffolds supporting 3T3 fibroblast proliferation	39

5. Conclusion	42
6. Acknowledgements	44
7. References.....	45

Abstract

Driven by the global trend in the sustainable economy development and environmental concerns, the exploring of plant-derived biomaterials or biocomposites for potential biomedical and/or pharmaceutical applications has received tremendous attention. Therefore, the work of this thesis is dedicated to high-value and high-efficiency utilization of plant-derived materials, with the focus on cellulose and hemicelluloses in the field of biomedical applications in a novel biorefinery concept.

The residual cellulose of wood processing waste, sawdust, was converted into cellulose nanofibrils (CNFs) with tunable surface charge density and geometric size through 2,2,6,6-tetramethylpiperidinyloxy (TEMPO)-mediated oxidation and mechanical defibrillation. The sawdust-based CNFs and its resultant free-standing films showed comparable or even better mechanical properties than those from a commercial bleached kraft pulp at the same condition, demonstrating the feasibility of producing CNFs and films thereof with outstanding mechanical properties from birch sawdust by a process incorporated into a novel biorefinery platform recovering also polymeric hemicelluloses for other applications. Thus, it is providing an efficient route to upgrade sawdust waste to valuable products. The surface charge density and geometric size of the CNFs were found to play key roles in the stability of the CNF suspension, as well as the gelling properties, swelling behavior, mechanical stiffness, morphology and microscopic structural properties, and biocompatibility of CNF-based materials (i.e. films, hydrogels, and aerogels).

The CNFs with tunable surface chemistry and geometric size was found promising applications as transparent and tough barrier materials or as reinforcing additive for production of biocomposites. The CNFs was also applied as structural matrices for the preparation of biocomposites possessing electrical conductivity and antimicrobial activity by in situ polymerization and coating of polypyrrole, and incorporation of silver nanoparticles, which make the material possible for potential wound healing application.

The CNF-based matrices (films, hydrogels, and aerogels) with tunable structural and mechanical properties and biocompatibility were further prepared towards an application as 3D scaffolds in tissue engineering. The structural and mechanical strength of the CNF matrices could be tuned by controlling the charge density of the nanocellulose, as well as the pH and temperature values of the hydrogel formation conditions. Biological tests revealed that the CNF scaffolds could promote the survival and proliferation of tumor cells, and enhance the transfection of exogenous DNA into the cells, suggesting the usefulness of the CNF-based 3D matrices in supporting crucial cellular processes during cell growth and proliferation.

The CNFs was applied as host materials to incorporate biomolecules for further biomedical application. For example, to investigate how the biocompatibility of a

scaffold is influenced by its mechanical and structural properties, these properties of CNF-based composite matrices were controlled by incorporation of different hemicelluloses (*O*-acetyl galactoglucomanan (GGM), xyloglucan (XG), and xylan) into CNF hydrogel networks in different ratios and using two different approaches. The charge density of the CNFs, the incorporated hemicellulose type and amount, and the swelling time of the hydrogels were found to affect the pore structure, the mechanical strength, and thus the cells growth in the composite hydrogel scaffolds. The mechanical properties of the composite hydrogels were found to have an influence on the cell viability during the wound healing relevant 3T3 fibroblast cell culture. The thus-prepared CNF composite hydrogels may work as promising scaffolds in wound healing application to provide supporting networks and to promote cells adhesion, growth, and proliferation.

Keywords

3D Cell culture, Aerogel, Biocomposites, Biorefinery, Cellulose nanofibrils, Hydrogel, Hemicelluloses, Sawdust, Scaffold, TEMPO oxidation, Tissue engineering, Wound healing.

Svensk sammanfattning

Utforskandet av vegetabiliska biomaterial eller biokompositer för potentiella biomedicinska och/eller farmaceutiska applikationer har fått en enorm uppmärksamhet som drivs av de globala trenderna för utveckling av hållbar ekonomi och ökad miljöhänsyn. Detta arbete är därför ägnat åt mervärdesprodukter och högeffektivt utnyttjande av vegetabiliska material, med fokus på cellulosa och hemicelluloser inom biomedicinska tillämpningar, enligt ett nytt bioraffinaderikoncept.

Den kvarvarande cellulosan i restprodukter från mekanisk sågverksindustri, d.v.s. sågspån, omvandlades till cellulosanofibriller (CNF) med avstämbar ytladdningstäthet och geometrisk storlek genom 2,2,6,6-tetrametylpiperidinyloxi (TEMPO) medierad oxidation och mekanisk defibrillering. De sågspånsbaserade cellulosanofibrillerna och fristående filmer av dessa visade jämförbara eller ännu bättre mekaniska egenskaper än motsvarande material från en kommersiellt blekt sulfatmassa vid samma betingelser. Dessa resultat framhäver potentialen att producera CNF och filmer därav med enastående mekaniska egenskaper från björksågspån som en del av en bioraffinaderiplattform där polymera hemicelluloser för andra tillämpningar också tas tillvara. På så sätt kan sågspånsavfall effektivt uppgraderas till värdefulla produkter. Ytladdningstätheten och den geometriska storleken hos CNF befanns vara i nyckelroller för stabiliteten hos suspensioner av CNF och gelbildningsegenskaperna, svällningsbeteendet, den mekaniska styvheten, morfologin och de mikroskopiska strukturella egenskaperna samt biokompatibiliteten hos CNF-baserade material (d.v.s. filmer, hydrogeler och aerogeler).

För CNF med avstämbar ytkemi och geometri fanns lovande applikationer som transparenta och starka barriärmaterial eller som förstärkningsmaterial för tillverkning av biokompositer. CNF användes också som strukturella matriser för framställning av biokompositer med elektrisk ledningsförmåga och antimikrobiell aktivitet genom in situ polymerisation och beläggning av polypyrrol och införlivande av silvernanopartiklar, som möjliggör användning i potentiella sårbehandlingsapplikationer.

De CNF-baserade matriserna (såsom filmer, hydrogeler och aerogeler) med kontrollerbara strukturella och mekaniska egenskaper samt biokompatibilitet vidareutvecklades mot en applikation som 3D-stödstrukturer i vävnadsrekonstruktion. Den strukturella och mekaniska styrkan hos CNF-matriserna kunde avstämmas genom att kontrollera laddningsdensiteten hos nanocellulosan, liksom också pH-värdet och temperaturen vid bildningen av hydrogelerna. Biologiska tester visade att CNF-stödstrukturerna kunde främja överlevnad och förökning av tumörceller samt öka transfektion av exogent DNA in i cellerna. Dessa resultat tyder på att CNF-baserade 3D-matriser kunde användas för att stödja viktiga cellulära processer under celltillväxt och -förökning.

CNF användes också som värdmaterial där biomolekyler inkorporerades för ytterligare

biomedicinska tillämpningar. Till exempel undersöktes hur biokompatibiliteten av en stödstruktur påverkas av dess mekaniska och strukturella egenskaper genom att inkorporera olika hemicellulosor (O-acetyl galaktoglukomannaner (GGM), xyloglukaner (XG), och xylaner) i CNF-hydrogel nätverket i olika förhållanden och med hjälp av två olika metoder. Laddningsdensiteten hos CNF-materialet, den inkorporerade hemicellulosans typ och mängd och svällningstiden för hydrogelerna befanns påverka porstrukturen, den mekaniska hållfastheten och därmed också celltillväxten i komposithydrogelernas stödstrukturer. De mekaniska egenskaperna hos hydrogelerna påverkade också cellernas livsduglighet under relevanta förhållanden för 3T3-sårlningsfibroblastceller. De sålunda framställda CNF-komposithydrogelerna kan fungera som lovande stödstrukturer i sårlningsapplikationer samt för främjande av cellernas vidhäftning, tillväxt och spridning.

Nyckelord

3D cellodling, aerogel, biokompositer, bioraffinering, cellulosa nanofibriller, hydrogel, hemicellulosor, sågspån, stödstruktur, TEMPO-oxidering, vävnadsrekonstruktion, sårlning

List of important abbreviations

3D	Three-dimensional
AFM	Atomic force microscopy
BC	Bacterial cellulose
BKP	Bleached kraft pulp
CNCs	Cellulose nanocrystals
CNFs	Cellulose nanofibrils
CNWs	Cellulose nanowhiskers (i.e. CNCs)
DAPI	4',6-diamidino-2-phenylindole
DP	Degree of polymerization
ECM	Extracellular matrix
HC	High charge
HP	Hot press
HPSEC	High performance size exclusion chromatography
GGM	Galactoglucomannans
LC	Low charge
NFC	Nanofibrillated cellulose (i.e. CNFs)
PBS	Phosphate-buffered saline
PPy	Polypyrrole
RMS	Root mean square
SEM	Scanning electron microscopy
SSA	Specific surface area
TEM	Transmission electron microscopy
TEMPO	2,2,6,6-tetramethylpiperidine-1-oxyl radical
WP	Wet press
XG	Xyloglucan

1. Introduction

1.1 Biorefinery

In line with the current focus on the sustainable economy, the new generation of biorefinery aims at the processing and utilization of renewable biomass for production of highly value-added chemicals, food, feed, fuels, energy, and materials in a sustainable way (Pfaltzgraff & Clark, 2014). Plant-derived biomass constitutes the most abundant renewable feedstock on earth and shows promising potential as an alternative to fossil resources.

A novel biorefinery aims at maximal preservation of the sophisticated structure and chemical nature of individual components in the plant-derived biomass during isolation for further tailoring into value-added products (Borrega et al., 2013). Sequential extraction of biomass enables the full utilization of valuable components in the biomass. For example, organic solvent extraction can be applied to isolate extractives; hot-water extraction can be carried out to extract non-cellulosic polysaccharides; cooking is a traditional way to separate lignin; and the residual cellulose can be a promising source for dissolving pulp and/or nanocellulose production (Kilpeläinen, 2012).

Comprehensive utilization of biomass in a novel biorefinery concept also requires the exploration of the valuable chemicals and/or materials from the plant, including some “waste” or by-products like branches, knots, barks, roots, leaves, and even sawdust. For example, the lignans with antioxidant and antitumor effects have been isolated from the “waste” knots of spruce (Willför et al., 2004); pectin with immunomodulating activities has been extracted from “waste” spruce bark (Le Normand et al., 2014); xylans with high molar mass have been extracted from “waste” sawdust (Kilpeläinen et al., 2014); and the residual cellulose in the sawdust after xylan extraction can be fabricated to nanocellulose (**Figure 1**).

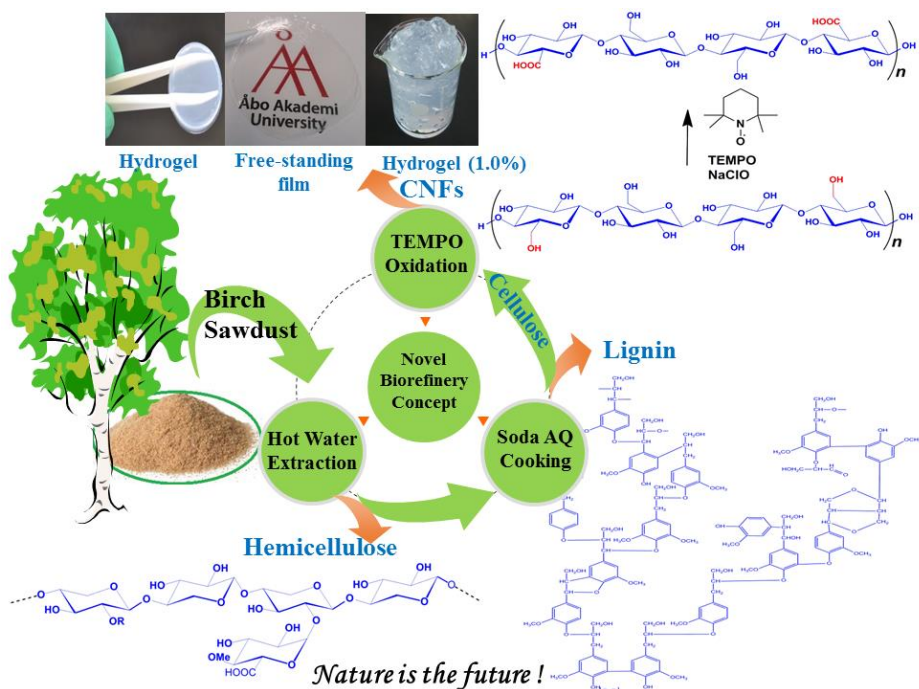


Figure 1. Sequential extraction of valuable components and production of cellulose nanofibrils (CNFs) from biomass in a novel biorefinery concept. Adapted with permission from paper II. Copyright (2014) Springer.

1.2 Nanocellulose

Cellulose, a homopolysaccharide composed of β -1,4-D-glucopyranose units, is an almost inexhaustible polymer available for biorefinery and other applications (Klemm et al., 2005). Cellulose molecules have strong tendency to form intramolecular and intermolecular hydrogen bond networks, which contributes to the interchain cohesion and formation of crystalline and amorphous regions (Klemm, 1998; Klemm et al., 2005).

In recent years, considerable attention has been paid to produce and utilize nanocelluloses, which have fascinating structural and chemical properties. Nanocelluloses, which mainly include cellulose nanocrystals (CNCs), cellulose nanofibrils (CNFs) (also terms as nanofibrillated cellulose, NFC), and bacterial cellulose (BC) have increasingly been investigated and applied in numerous areas, such as papermaking, oil drilling, medicine, and pharmaceuticals (Gandini et al., 2015; Klemm et al., 2011). In general, nanocelluloses can be prepared via mineral acid hydrolysis and mechanical defibrillation approaches. Enzymatic and chemical pretreatments can be used to assist the mechanical processing and/or to introduce surface charges, as summarized in Figure 2 and detailed in the text below. Recently, recyclable solid organic acid, oxalic acids, has been reported to prepare CNCs and CNFs with high thermal stability (Chen et al., 2016).

Currently (by the end of 2015), production of nanocellulose has been commercialized by a few entities. Among them, the Paperlogic™, Borregaard, and American Process focus on the CNF production and with current or announced capacity of 2000, 500, 500 kg/day respectively. The CelluloForce and American Process focus on the CNC production and with current or announced capacity of 1,000 and 500 kg/day respectively (Miller, 2015). Numerous research institutes, universities, and pulp mills are also producing nanocellulose in different forms in pilot or pre-commercial scale all over the world.

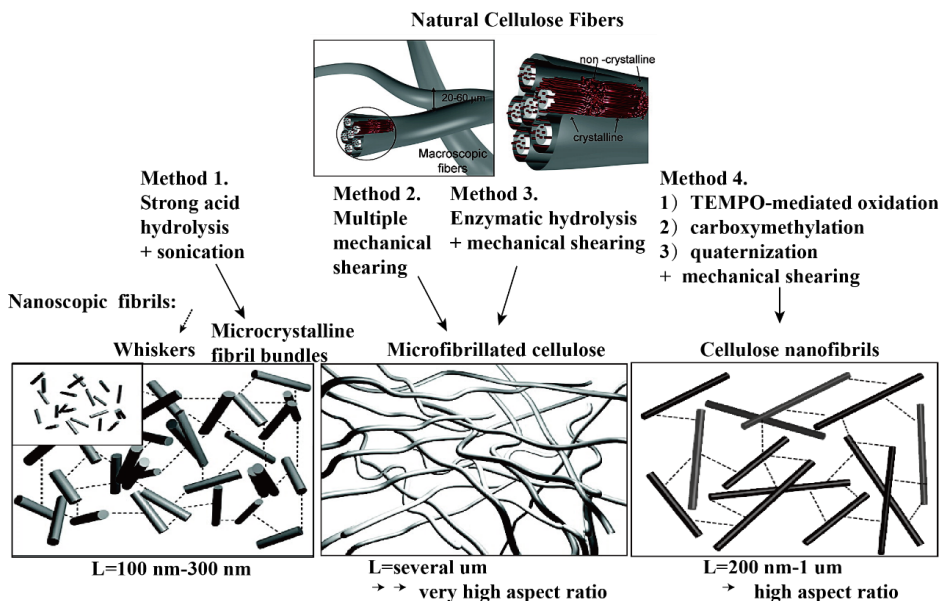


Figure 2. Four methods for preparing nanoscale cellulosic fibrils. Adapted and modified from (Pääkkö et al., 2007; Saito et al., 2006; Wågberg et al., 2008). Copyright (2007) American Chemical Society.

1.2.1 Cellulose nanocrystals (CNCs)

CNCs, earlier termed as cellulose nanowhiskers (CNWs), are mostly prepared by acid hydrolysis of cellulose fibers or microcrystalline cellulose to remove the amorphous parts of the raw materials (**Figure 2**, method 1) (Nickerson & Habrle, 1947). The resultant rigid rod-like nanocrystals with dimensions of 4-25 nm in diameter and a few hundred nanometers in length show excellent modulus of elasticity (~ 150 GPa), low thermal expansion coefficient ($\sim 10^{-7}$ K $^{-1}$), and intense macroscopic birefringence (Marchessault et al., 1959; Nishino et al., 2004; Revol et al., 1998); and thus have been applied as mechanical reinforcing agents for biocomposite preparation, for security paper and packaging materials (Popa, 2011).

1.2.2 Cellulose nanofibrils (CNFs)

CNFs is manufactured by defibrillation of cellulose fibers applying high shear

forces to expose the fibers' substructural fibrils and microfibrils (**Figure 2**, method 2) (Turbak et al., 1983). Enzymatic and/or chemical pretreatments (e.g. TEMPO-mediated oxidation) can be applied to facilitate defibrillation and to reduce the energy consumption during mechanical processing (**Figure 2**, method 3 and method 4), and also to introduce active functional chemical groups (**Figure 2**, method 4), such as carboxyl groups, aldehyde groups, carboxymethyl groups, and trimethylammonium chloride groups for further modification and application (Fukuzumi et al., 2009; Pei et al., 2013; Wågberg et al., 2008). The disintegrated fibrils, with a diameter of 5-20 nm and a length of several hundred nanometers to a few micrometers, are highly entangled and tend to form a hydrogel, which shows promising applications in biomedicine, pharmaceuticals, and cosmetics (Lin & Dufresne, 2014; Popa, 2011).

1.2.3 Bacterial cellulose (BC)

BC is produced by cultivation of various bacterial strains, e.g. the *Acetobacter xylinum* (or *Gluconoacetobacter xylinus*), in culture media where the cellulose is produced by cellulose-synthesizing complexes of bacteria between the outer and cytoplasmic membrane (Brown, 1886; Vandamme et al., 1998).

BC possesses unique properties, including high crystallinity (>85%), high degree of polymerization (up to 10,000), high mechanical strength (Young's modulus of BC sheets >15 GPa), high water absorption capacity, and ultra-fine dimension (2-4 nm in diameter) and 3D network structure (Czaja et al., 2004; Kamel, 2007; Vandamme et al., 1998; Yamanaka et al., 1989; Yoshinaga et al., 2014).

Current applications of BC include utilization in food industry as dietary fiber, in biomedicine as artificial skin for wound healing and as artificial blood vessels for microsurgery, in cosmetics as moistening masks, and in fiber-based biocomposites manufacture as reinforcement materials (Klemm et al., 2006; Klemm et al., 2001; Nogi et al., 2006; Okiyama et al., 1993; Yano et al., 2005).

1.3 Hemicelluloses

Hemicelluloses, the second most abundant polysaccharides in nature after cellulose, mainly include xylans, glucomannans, arabinans, galactans, and glucans (Popa, 2011). In plant cell walls, hemicelluloses are closely associated with cellulose and lignin, and account for up to 50% of the total mass of the biomass, and therefore have been viewed as an immense renewable resource of biopolymers (Ebringerová et al., 2005).

Of increasing interest in a broad spectrum of applications in different areas, such as food and feed, cosmetic, pharmacy and medicine, is the fact that hemicelluloses are readily available, biodegradable, nontoxic, capable of chemical modifications, and bioactive in some cases (Ebringerová et al., 2005). Chemical modifications of hemicelluloses by graft polymerization, cross-linking, (regioselective) oxidation,

reduction, esterification, etherification, and partial hydrolysis further open opportunities for various applications (Sun et al., 2003).

1.4 Biocomposites

1.4.1 Nanocellulose-based biocomposites

Biocomposites are combinations of two or more components, with one or more phase(s) derived from a biological origin, that are mixed together to produce materials with entirely different or enhanced thermal, mechanical, electrical, and/or biological properties from those of the individual components (Ali & Hongbo, 2014; Fowler et al., 2006; John & Thomas, 2008).

Nanocellulose-based biocomposites, also termed as cellulose nanocomposites, consist of nanocelluloses (including CNFs, CNCs, and BC) as host-substrate to manufacture structural and functional biocomposites (Ali & Hongbo, 2014). By incorporation of different components such as synthetic polymers, biomacromolecules, and even living cells, and by integration of various material processing techniques, nanocellulose-based biocomposites with unique optical, electrical, mechanical, and biological properties in the form of films, particles, hydrogels, and aerogels have been developed for packaging, electronic devices, and biomedical applications (Dax et al., 2015; Fu et al., 2013; Nogi et al., 2009; Shi et al., 2013; Wan et al., 2006; Yano et al., 2005).

1.4.2 Nanocellulose-based biomaterials for biomedical applications

The inherent properties of nanocelluloses, such as nontoxicity, biocompatibility, biodegradability, excellent structural strength and stiffness, and thermal stability endow them good candidates for biomedical applications such as medical implants, tissue engineering, wound healing/dressing, and drug delivery (Jorfi & Foster, 2015; Klemm et al., 2011; Oksman et al., 2009).

Scaffolds in engineered tissue are to mimic the extracellular matrix (ECM) in native tissues (Chan & Leong, 2008). The ECM provide a microenvironment with proper structure, elasticity, binding sites for cell surface receptors and signal factors for cell proliferation, adhesion, migration, and differentiation (Carletti et al., 2014; Hrebikova et al., 2015). Therefore, the functions of the ECM to be mimicked include: porous architecture supporting cells to reside and allowing nutrient and metabolite transportation; sufficient mechanical and shape stability to provide proper dynamic signaling cues; necessary bioactive cues, e.g. growth factors, for cells to respond to microenvironment; cyto- and tissue compatibility for both *in vitro* culture and *in vivo* implantation (Chan & Leong, 2008; Lanza et al., 2007; Muschler et al., 2004; Nakayama et al., 2014).

The nanocellulose-based biocomposites in tissue engineering for replacing or restoring damaged or diseased tissue are supposed to work as scaffolds or matrices

to support crucial cellular activities, such as cell attachment, proliferation, and subsequent tissue formation (Czaja et al., 2007; Joshi et al., 2016; Moroni et al., 2006). BC-based biocomposites have been intensively studied for tissue engineering application. For example, hydroxyapatite (HA)/BC nanocomposite scaffolds were found potency applicable in bone tissue engineering to modulate the proliferation and osteoblastic differentiation of human bone marrow stromal cells (Fang et al., 2009), and in the bone regeneration of rat with bone defects (Saska et al., 2011). BC/collagen biocomposites (Luo et al., 2008; Saska et al., 2012), BC/heparin biocomposites (Wan et al., 2011), and BC/polyvinyl alcohol biocomposites (Millon et al., 2008; Wang et al., 2010) have been prepared for potential use in various tissue engineering applications. Except the BC, other nanocellulose-based biocomposites, such as CNC (Dugan et al., 2013a; Dugan et al., 2013b; Dugan et al., 2010), CNFs (Bhattacharya et al., 2012; Malinen et al., 2014; Syverud et al., 2011; Syverud et al., 2015), CNFs/alginate biocomposites (Markstedt et al., 2015), CNFs/polyaniline biocomposites (Leppänen et al., 2013), CNFs/gelatin/ β -tricalcium phosphate biocomposites (Sukul et al., 2015), and CNFs/nanochitin biocomposites (Torres-Rendon et al., 2015) have also found promising applications in tissue engineering.

Wound healing is a multi-factorial physiological process (Demir & Cevher, 2011). Healing of different types of wounds and burns require different materials and treatments. However, there are a few general characteristics can be taken into consideration to design a wound or burn dressing material. The ideal wound dressing material should mimic the physiochemical, mechanical, biological, and antimicrobial functions of the extracellular matrix (Ramanathan et al., 2016). For example, the materials should possess sufficient moisture and oxygen permeability, high exudate absorption capacity, suitable elasticity and mechanical strength, non-toxic and non-antigenic properties, efficient inhibition of bacterial invasion, easy application, biodegradability, and compatibility with topical therapeutic agents (Demir & Cevher, 2011). Traditional dressing like gauze and gauze-cotton composites, biomaterial-based dressing like allografts, xenografts, and tissue derivatives, and various artificial dressings in the form of film/membrane, foam, gel, composite, and spray, are widely used for wound or burn treatment to provide optimum healing conditions (Stashak et al., 2004).

Owing to the high water-holding capacity, flexibility, porosity, and elasticity features of nanocelluloses, the nanocelluloses and their biocomposites are recognized as excellent wound healing/dressing materials (Popa, 2011). BC-based materials or biocomposites, such as XCell[®], Bioprocess[®], Biofill[®], Suprasorb X[®], and Dermafill[®] are already commercialized for wound healing/dressing (Petersen & Gatenholm, 2011; Portal et al., 2009). Other nanocelluloses, especially the CNFs (with or without TEMPO-mediated oxidation), have also been extensively studied for potential wound healing in recent years. CNFs has been shown to be non-cytotoxic (Alexandrescu et al., 2013; Chinga-Carrasco & Syverud, 2014), to impair

growth of common wound bacteria (Powell et al., 2016), to support the wound healing relevant fibroblast cells adhesion, survival, proliferation, and gene expression (Alexandrescu et al., 2013; Hua et al., 2014; Pereira et al., 2013), which are all suitable characteristics for wound healing applications. Recently, glutaraldehyde crosslinked CNFs was studied to deliver human adipose mesenchymal stem cells into chronic wounds to reduce inflammation and to promote wound healing (Mertaniemi et al., 2016).

Nanocellulose-based drug delivery systems have been intensively studied thanks to their excellent properties, such as the high specific surface area, which enables a high drug load, various chemical modification possibilities, which broaden the range of the drugs to be loaded, and different materials processing techniques that allow the tuning of the drug release profiles (Habibi, 2014; Plackett et al., 2014). Nanoelluloses have been prepared in the form of suspensions, hydrogels, freeze-dried aerogels, spray-dried microparticles, films, or tablets to deliver drugs for controlled release (Kolakovic et al., 2012a; Kolakovic et al., 2012b; Lin & Dufresne, 2014; Valo et al., 2013), to deliver chemotherapeutic agents to cancer cells (Dong et al., 2014), and to deliver biomacromolecules such as albumin (Müller et al., 2013), growth factors (Lin et al., 2011b), genes (Anirudhan & Rejeena, 2014), and cells (Mertaniemi et al., 2016).

2. Hypothesis and objectives of the work

Driven by the global trend in the sustainable economy development and environmental concerns, the aim of this work was a comprehensive utilization of renewable plant-derived materials, with the focus on cellulose and hemicelluloses, in the field of biomedical applications in a novel biorefinery concept.

The first objective was the preparation of cellulose nanofibrils (CNFs) from biomass in a novel biorefinery concept, i.e. integration of hot-water extraction of hemicelluloses, lignin separation, and CNFs production. The surface chemistry and geometric size of the CNFs were assumed to be controlled during production and these properties were supposed to contribute to different properties of the CNF-based materials.

The second objective was to utilize the CNFs as host-substrate to incorporate various biomolecules such as polysaccharides, proteins, genes, live cells, and drugs to prepare biocomposites for potential biomedical applications, such as tissue engineering and wound healing. The CNF-based materials in the forms of film, hydrogel, or aerogel are supposed to work as supporting networks, carriers, reinforcement agents, and potential biochemical and mechanical cues of cellular activities in biomedical applications. In order to meet various requirements of the materials in biomedical applications, the properties of the CNF-based materials were assumed to be tuned by controlling the chemical and physical properties of the CNFs itself, by introducing bioactive molecules, and by applying different material shaping and processing techniques.

3. Materials and methods

3.1 Materials

A birch sawdust pulp (initial kappa number: 4.7, brightness: 59.9 % ISO) after hot-water extraction, soda-AQ delignification, and a four-stage elemental chlorine free bleaching (hemicellulose content: 8.6%) (**Paper II**); a commercial bleached birch kraft pulp (BKP) with hemicellulose content of 18.6% (**Paper II and Paper III, Paper IV**); and a spruce dissolving pulp with hemicellulose content of 4.9% (**Paper V**) were used as starting materials to prepare CNFs.

Xylan was extracted from birch sawdust using pressurized hot water flow-through extraction, with sodium acetate buffer at pH 4.0, at 160 °C for 30 min (Kilpeläinen et al., 2013), and was sequentially purified by ethanol precipitation (9:1, v/v) and solvent washing (methanol, 2-propanol, and methyl *tert*-butyl ether). Xyloglucan (XG) from commercial tamarind seeds (Innovasynth Technologies Ltd.) was purified prior to application as described before (Xu et al., 2012). *O*-acetyl galactoglucomannan (GGM) was prepared from the spruce thermomechanical pulp by a laboratory-scale method modified from Willför et al. (Willför et al., 2003; Xu et al., 2010).

All chemicals were purchased from Sigma-Aldrich, MERCK, or VWR and used without further purification.

3.2 Preparation methods

3.2.1 Preparation of CNFs (**Paper II, III, IV, V**)

The CNFs preparation procedures were optimized from Saito and Isogai's report (Saito & Isogai, 2004). One gram of cellulose fibers (bleached sawdust pulp in **paper II**, bleached birch kraft pulp in **paper III** and **paper IV**, and spruce dissolving pulp in **paper V**) were dispersed in 60 mL distilled water and stirred for 4.0 h at room temperature. The TEMPO (16 mg, 0.1 mmol/g fiber) and NaBr (100 mg, 1.0 mmol/g fiber) were dissolved in 40 mL distilled water, and were mixed with the fiber suspension. The pH of the pulp slurry was adjusted to 10.0 by the addition of 0.5 M NaOH. The oxidation was started by dropwise adding the NaClO solution (12% wt. active chlorine). The NaClO dosage (5-10 mmol/g fiber) and the reaction time were controlled to tune the surface charge density and geometric size of the final product. The total volume of the NaClO was added within one-third of the designated reaction time and the pH was maintained at 10.5 by adding 0.5 M NaOH. The oxidized fibers were precipitated in ethanol with a ratio of 1:3 (v/v) and thoroughly washed with deionized water by filtration (**paper II**) or centrifugation (**paper III, paper IV, and paper V**), until the conductivity of the filtrate was below 4.5 μ S/cm. The oxidized fibers at a consistency of 0.5% were fibrillated by a domestic blender (OBH Nordica 6658, Denmark) for 5 min at an output of 300 W (**paper II, paper III, and paper IV**), or were homogenized with

a Rannie 15 type 12.56x homogenizer operated at 600 bar and 1000 bar for the first and second pass (**paper V**), respectively. The CNFs was stored at 4.0 °C before further use.

3.2.2 Preparation of CNF free-standing films (**Paper II, III, IV**)

CNF free-standing films were prepared via filtration of the CNF dispersion (0.1%, wt., 300 mL) on a nylon membrane filter (0.2 µm pores, Ø= 90 mm) with a funnel (Sterlitech, USA) under vacuum. The filter cake was dried in vacuum desiccator at 40 °C at a pressure of 88 mbar for 4.0 h (**Paper II, Paper III**), or was wet pressed (WP) between filter papers under a pressure of 88 mbar to blot water (**paper IV**) until dry, or was hot pressed (HP) after the WP preparation but at 80 °C and at a pressure of 2.3 bar (Scan CM 64:00) for 20 min (**paper IV**).

3.2.3 Preparation of CNF polypyrrole silver composite films (CNF-PPy) (**Paper III**)

To prepare the CNF-PPy biocomposite films (**Paper III**), the pyrrole (10 mM) was first oxidized with AgNO₃ or iron(III) nitrate (Fe(NO₃)₃) in a mole ratio of 2.3 (oxidant : pyrrole), or their mixtures of various composition in 0.5 wt % aqueous CNF dispersions. After mixing the suspensions (CNFs, pyrrole, and oxidants), the mixtures were left unstirred at room temperature for 24 h or for 1 week when the oxidation was done. The final suspensions were subjected to film preparation as described above.

3.2.4 Preparation of CNF hydrogels and aerogels (**Paper IV**)

CNF hydrogels were prepared by swelling the CNF films in swelling media (Milli-Q water, HCl or NaOH solutions) at the predetermined temperature and pH for 24 h. To prepare the CNF aerogels, and to maintain the porous structure, solvent exchange of the CNF hydrogels was carried out step-wise with ethanol (25%, 50%, 75%, 95%, and 99.5%), followed by solvent exchange with *tert*-butanol for 24 h. The samples were frozen using liquid nitrogen for 30 min followed by freeze-drying for 72 h under a pressure of 0.1 mbar.

3.2.5 Preparation of all-polysaccharide composite hydrogels (**Paper V**)

To prepare the all-polysaccharide composite films, the hemicelluloses (GGM, XG, and xylan) were dissolved in Milli-Q water (1 g/L) and mixed with the CNF suspension in different weight ratios (90:10, 70:30), giving a final concentration of 0.1 g/L. The suspension was stirred at 65 °C for 5 h (Stevanic et al., 2014), followed by film preparation via vacuum filtration as described above.

The all-polysaccharide composite hydrogels were prepared by following two approaches, i.e. pre-sorption and in-situ sorption methods.

Method I: The pre-sorption refers to the adsorption of hemicellulose into the CNF networks by hot mixing before composite film preparation (Prakobna et al., 2015a;

Stevanic et al., 2014), and the corresponding hydrogels were obtained by swelling of the composite films in Milli-Q water at room temperature for 24 h.

Method II: The in-situ sorption denotes the simultaneous formation of the CNF hydrogel during swelling and the adsorption of hemicelluloses into the hydrogel networks. The pure CNF films were swollen in different hemicellulose solutions with various concentrations (5.0 g/L and 0.5 g/L) at room temperature for 24 h to form the corresponding composite hydrogels.

3.3 Biotest methods

3.3.1 Antimicrobial property of films (Paper III)

The antimicrobial test of the CNF-PPy biocomposites was performed against both Gram-positive (*Listeria monocytogenes* ATCC 7644, *Staphylococcus aureus* 298) and Gram-negative bacteria (*Salmonella infantis* EELA 72), and also against yeast (*Candida albicans* EELA 188). All Gram-positive bacteria were grown in Tryptone soy agar or broth at 37 °C, and the *Candida* was grown in Sabouraud dextrose agar or broth at 30 °C. The biocomposite films (approximately 1 cm²) were placed on top of each agar plate. Overnight cultures of each bacterium were mixed with 0.4% bacteriological agar and poured on top of the agar plates as an overlay layer, also covering the biocomposite films. The plates were subsequently incubated for 24 h at their respective temperatures. The antimicrobial activity was evaluated by measuring the growth inhibition zones around the films.

3.3.2 Biocompatibility test of CNF-based scaffolds (Paper IV, V)

In paper IV, cell culture on the standard platform (24-well plate, glass slides (Mock) as control) and CNF matrices (film and aerogel) was carried out using epithelial-derived Hela cells and hematopoietic-derived Jurkat cells for *in vitro* assessment of the common cellular functions (e.g. cell attachment, viability, and proliferation) on scaffolds. Sterilization of all the CNF matrices was carried out by exposing to UV radiation for 30 min. Hela cells and Jurkat cells were seeded onto the CNF matrices by dropping the cell suspension on the film or aerogel surface at a seed density of 5×10^5 cells per piece film (5×5 mm \times 45 μ m, length \times width \times thickness) or aerogel in the 24-well plate. Hela cells were maintained with DMEM (4.5 mM glucose) supplemented with 2 mM L-glutamine, 100 IU/mL penicillin and streptomycin, and 10% heat-inactivated FBS (Invitrogen). Jurkat cells were cultured in RPMI medium with the same supplements as for the Hela cells. All cells were incubated with 5% CO₂ at 37 °C and 95% humidity. The medium was renewed daily for three days.

For *in vitro* proliferation assays, cells were seeded on the CNF matrices in 96-well cell plates and placed in the integrated incubator on Cell IQ live cell imaging and automated analysis system instruments (CM Technologies, Tampere, Finland). The samples were imaged automatically at regular 6 h intervals with kinetic

proliferation data for 72 h. Quantification of the number of live, dead, and dividing cells was extracted from the phase contrast image series and proliferation videos were made based on the corresponding data extraction.

In paper V, the NIH 3T3 fibroblast cells were cultured on the CNF composite hydrogels and a mock platform (glass slide) as a control in a 24-well plate to assess the biocompatibility of the matrices. Briefly, composite films and pure CNF films (5×5 mm×45 μm, length × width × thickness) were swollen in Milli-Q water and hemicellulose solutions, respectively, to form 3D hydrogel matrices for 24 h, followed by equilibration in the cell culture media for 24 h. UV radiation was used for sterilization of the hydrogels for 30 min. The NIH 3T3 fibroblast cells were seeded onto the hydrogel matrices at a density of 3×10^5 cells per piece of hydrogels in a 24-well plate. The NIH 3T3 cells were cultured with DMEM supplemented with 200 mM L-glutamine, 1000 IU/mL penicillin and streptomycin, and 10% Inactivated FBS. All cells were incubated at 37 °C with 5% CO₂ and 95% humidity.

3.4 Analytical methods

3.4.1 Molar mass measurement of hemicelluloses (Paper V)

The weight-average molar mass (M_w) of the hemicelluloses (XG, GGM, and Xylan) was determined using high performance size exclusion chromatography (HPSEC) with a multi-angle laser light scattering (MALLS) detector (miniDAWN, Wyatt Technology, Santa Barbara, USA) and a refractive index (RI) detector (Shimadzu Corporation, Japan). Separation of the hemicelluloses was done with a two-column in series system, 2 × Ultrahydrogel™ linear 300 mm x 7.8 mm column (Waters, Milford, USA). The dn/dc value of 0.150 mL/g was applied for XG and GGM, and the value of 0.146 mL/g was applied for xylan (Michielsen, 2003).

3.4.2 Charge density measurement of CNFs (Paper II, III, IV, V)

Conductometric titration was applied to determine the carboxylate content of the CNFs. To 50 mg of CNFs (0.1%, w/v), 2.0 mL of 0.1 M HCl and 1.0 mL of 50 mM NaCl were added. Then the slurry was stirred for 90 min before titration. The mixture was titrated with 0.1 M NaOH at the rate of 0.1 mL/min and the carboxylate content of the sample was calculated from the conductivity and pH curves (Araki et al., 2000). In **Paper IV** and **Paper V**, low charge CNFs (LC CNF) and high charge CNFs (HC CNF) were used.

3.4.3 Transmission Electron Microscopy (TEM) imaging of CNFs (Paper II, III, IV, V)

The CNF suspension at a concentration of 0.05% was deposited on a copper grid/carbon film, followed by staining with 2% uranyl acetate for 40 s. Excess solution was blotted with a filter paper and the sample was allowed to stand for drying. TEM images were captured using a JEM-1400 Plus TEM instrument

(JEOL, Japan) operated at an accelerating voltage of 80 kV. The geometric size of the CNFs was obtained by analyzing the CNFs' TEM images using the iTEM program (Olympus Soft Imaging Solution, Germany).

3.4.4 Ultraviolet-Visible (UV-Vis) transmittance measurement of films (Paper II, V)

Transmittance spectra (300–1000 nm) of the CNF suspension at a concentration of 0.1% were measured using a UV-Vis spectrometer (Perkin Elmer Lambda 40) (**Paper II**). The UV-Vis transmittance spectra of the CNF films and CNF-hemicellulose composite films were recorded with a UV-Vis spectrophotometer (Cary 300 Conc, Varian) (**Paper V**).

3.4.5 Fourier Transform Infrared Spectroscopy (FTIR) spectroscopy of films (Paper III, IV)

Before the FTIR measurement, the CNF suspension was acidified with 0.1 M HCl for 3 h, and then freeze-dried after thorough washing (Fujisawa et al., 2011). The FTIR spectra of the CNF samples were recorded using an FTIR spectrometer (Bruker ALPHA) in ATR module in the range of 400–4000 cm^{-1} with a 4 cm^{-1} resolution, and with an accumulation of 64 scans (**Paper IV**).

The FTIR-ATR spectra of the CNF-PPy composite films were recorded using a Harrick's VideoMVP single reflection diamond ATR accessory. The composite films were pressed against the diamond crystal attached to the Bruker IFS 66S spectrometer equipped with a DTGS detector. A total of 32 scans were recorded for each spectrum with a resolution of 4 cm^{-1} (**Paper III**).

3.4.6 Electrical conductivity measurement of CNF-PPy composite films (Paper III)

The electrical conductivity of the samples was characterized by 4-point probe measurements, in a linear configuration, having a tip spacing of 1.82 mm. A suitable bias current of 10^{-10} to 10^{-3} A was applied over the sample and the corresponding voltage was measured. The conductivity of the samples was calculated using finite-size corrections (Smits, 1958).

3.4.7 Swelling degree measurement of films (Paper IV, V)

Water uptake of CNF free-standing films in swelling media (**Paper IV**, Milli-Q water; **paper V**, hemicellulose solutions) to form hydrogels was monitored by measuring the amount of water uptake with a gravimetric method. Films were immersed into the swelling media and soaked at a predetermined temperature and pH. At a given time, the swollen film (hydrogel) was weighed after taken out from the swelling media and removing the excess water from the surface with blotters. The swelling degree was calculated according to equation (1):

$$\text{Swelling degree } X \text{ (g/g)} = (X_{\text{wet}} - X_{\text{dry}}) / X_{\text{dry}}, \quad (1)$$

Where, X_{wet} and X_{dry} denote the weight of the films in wet or dry condition, respectively.

3.4.8 Topography and morphology analysis of films with laser profilometry (Paper V)

The topography and morphology of the pure CNFs and CNF-hemicellulose composite films were assessed with laser profilometry (Lehmann, Lehman Mess-Systeme AG, Baden-Dättwil, Germany). A strip of 10 mm × 10 mm films was coated with a layer of gold for laser profilometry topography imaging. Ten surface images from both sides of each film were acquired and bandpass filtered (FFT filter, ImageJ program) for film surface topography quantification.

3.4.9 Atomic Force Microscope (AMF) imaging of films (Paper V)

The AFM images of the pure CNF and CNF-hemicellulose composite films were captured using a Multimode AFM (with Nanoscope V controller) Digital Instruments in ScanAsyst mode (peak force tapping mode) at room temperature with a resolution of 1.95 nm/pixel.

3.4.10 Scanning Electron Microscope (SEM) imaging of aerogels (Paper IV, V)

To visualize the porous structure of the hydrogels, the hydrogel samples (cubic, 5 × 5 × thickness, mm) were frozen using liquid nitrogen for 30 min followed by freeze-drying for 72 h. The resultant aerogels were sputter-coated with carbon (**Paper IV**) or with gold (**Paper V**). SEM images of the cross-section of the aerogels were captured using a scanning electron microscope (LEO Gemini 1530, Germany) equipped with an UltraDry Silicon Drift Detector (Thermo Scientific, USA) at an accelerating voltage of 5kV (**Paper IV**), or using a Hitachi S-5500 electron microscope at an acceleration voltage of 5 kV (**Paper V**).

3.4.11 Confocal laser scanning microscopy imaging of CNF-based scaffolds (Paper IV, V)

Hela cells and Jurkat cells (**Paper IV**) that were incubated with CNF matrices or the control glass slide (Mock platform) were collected after 72 h incubation and then analyzed for cell viability. For the detection of permeabilized (dead) cells, the cells were trypsinized and resuspended in 50 µg/mL Propidium Iodide (PI) in PBS for 10 min at room temperature, then analyzed by a FACSCalibur flow cytometer (FSC, BD Pharmingen).

After 24 h cell culture, the NIH 3T3 fibroblast cells (**Paper V**) were fixed with 4.0% paraformaldehyde and a mixture of acetone and methanol (1:1). Triton X (0.2%) in PBS was used to permeabilize the cell membranes, and the 10% FBS in Triton X and PBS was used for blocking for 2 h. The cells were stained with Alexa Fluor 488 overnight, and counterstained with DAPI for 10 min before mounting on glass

slides. Confocal images were acquired on a Zeiss LSM780 confocal laser scanning microscope (Carl Zeiss, Inc.).

3.4.12 Tensile/compressive strength measurement of films, hydrogels, and aerogels (Paper II, III, IV, V)

The mechanical strength of the pure CNF films and CNF-PPy biocomposite films with 5 mm width were determined using an Instron universal testing machine (Instron-33R4465, (Instron Corp., High Wycombe, England)) equipped with a static load cell of 100 N and an initial grip distance of 20 mm (**Paper II, III**). A pre-run was done with the tensile tester until 0.1 N load was reached. Ten specimens from three replicate films of each sample were tested after conditioning at 50% RH and 23 °C.

For **paper IV**, the mechanical properties of the CNF hydrogels and their resultant aerogels were characterized using a TA Instrument Dynamic Mechanical Analyzer Q800 (New Castle, USA) operated in compression mode. The cylindrical hydrogel ($\varnothing = 12.85$, mm) or the cubic aerogel ($3 \times 3 \times$ thickness, mm) were tested at a compression rate of 1.0 N/min by using load cells of 5.0/10 N. A preload of 0.05 N was applied before compression testing. At least five parallel hydrogel and aerogel specimens were measured for each sample, and the results were calculated and reported as mean \pm S.D. The elastic modulus of the hydrogel and aerogel was obtained by linear fitting of the elastic region of the stress-strain curves (Ohya et al., 2001).

For **paper V**, a texture analyzer (TA.XT.-Plus Texture Analyzer, Surrey, UK) was used to determine the compressive strength of the hydrogels (cubic, $5 \times 5 \times$ thickness, mm). The texture analyzer was operated at a compression speed of 0.1 mm/s by using a 1.0 kg load cell. A preload of 1.0 g was applied before compression testing. At least five parallel hydrogel specimens were measured for each sample, and the results were calculated and reported as mean \pm S.D.

3.4.13 Pore property analysis of aerogels (Paper IV)

The specific surface area (SSA) of the CNF aerogels was determined by N₂ adsorption using a Sorptomatic 1900 (Carlo erba instruments, UK), and calculated by the Brunauer-Emmett-Teller method (Brunauer et al., 1938). The mesopore specific volume was calculated by the Barrett-Joyner-Halenda method (Barrett et al., 1951). The aerogel samples were degassed and dried at 120 °C for 3.0 h prior to measurement. The apparent density (ρ^*) of the aerogels was determined by measuring the mass (± 0.01 mg) and the geometric dimensions of the samples, the porosity of the aerogels was calculated according to equation (2). The skeletal density of cellulose ($\rho_c = 1.50$ g/cm³) used in the nitrogen adsorption measurements was verified employing Helium pycnometry.

$$\text{Porosity} = (1 - \rho^* / \rho_c) \times 100\% \quad (2)$$

4. Results and discussion

4.1 Summary and overview of the thesis work

The work of this thesis aimed at comprehensively utilizing components of plant-derived materials, with the focus on cellulose and hemicelluloses, in the field of biomedical applications in a novel biorefinery concept. As shown in **Figure 3**, the nanocellulose with tunable surface chemistry and geometric size has found promising applications as transparent and tough barrier materials (**Paper II**), as structural matrices for tailoring antimicrobial and electroconductive biocomposites (**Paper III**), as biocompatible 3D scaffolds in tissue engineering (**Paper IV**), and also as host materials to incorporate biomolecules such as hemicelluloses for strength reinforcing and for potential wound healing application (**Paper V**). Hemicelluloses, the second most abundant polysaccharides after cellulose, were used as additives to tune the properties of the nanocellulose hydrogels for potential wound healing applications (**Paper V**).

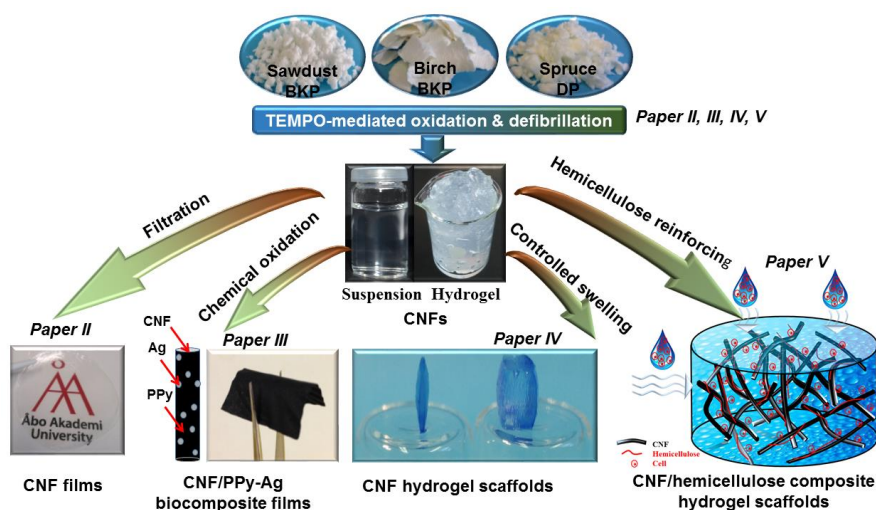


Figure 3. Overview of the thesis work.

4.2 Preparation of CNFs from sawdust in an integrated biorefinery process (Paper II)

Utilization of renewable biomass for the production of value-added products in the biorefinery platform has received tremendous attention in both academic research and industrial production (FitzPatrick et al., 2010). The scheme in **Figure 4** demonstrates the feasibility of producing CNFs and films thereof with high mechanical properties, and the corresponding hydrogels with high swelling degree from a wood “waste”, i.e. birch sawdust, by a process incorporated into a novel biorefinery platform. After sequential extraction of hemicelluloses and lignin, the residual cellulose in the sawdust was converted to CNFs through the TEMPO-mediated oxidation approach, which provided an efficient way to upgrade the sawdust “waste”.



Figure 4. Scheme of the process to prepare CNFs from sawdust in a novel biorefinery concept.

4.2.1 Preparation and characterization of CNFs from sawdust fiber

To prepare CNFs with different properties, the sawdust fiber and a reference bleached kraft pulp (Ref. BKP) were oxidized by the TEMPO/NaBr/NaClO system with different reaction time and oxidant dosages (**Figure 5**). The reaction equilibrium was reached at 4.0 h for the reference BKP and 6.0 h for the sawdust fiber at the NaClO dosage of 5 mmol/g fiber, and at 9.5 h for both starting materials at the NaClO dosage of 10 mmol/g fiber. Extension of the reaction time further increased the carboxylate content but may cause a low yield of the product due to the degradation (Saito & Isogai, 2004), and a lower DP of the resultant CNFs (**Table 1**).

The charge density (carboxylate content) of the CNFs was found to affect the stabilization of its suspension. A strong electrostatic repulsion allows the cellulose nanofibrils to be well-dispersed in water (Saito et al., 2006). As shown in **Figure 6**, the higher the CNF charge density, the clearer the suspension's appearance is, and the higher the light transmittance is.

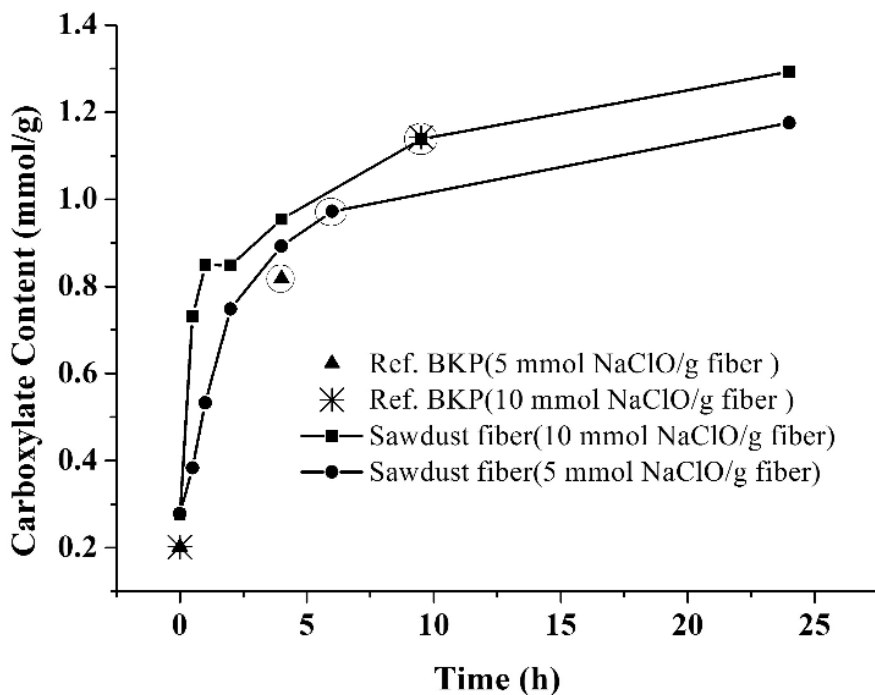


Figure 5. The course of carboxylate content of CNFs versus time of TEMPO-mediated oxidation of bleached birch kraft pulp (Ref. BKP) and sawdust fibers with different NaClO dosages. Circled points are the equilibrium points when the pH of the reaction mixture remained stable. Adapted with permission from Paper II, Copyright (2014) Springer.

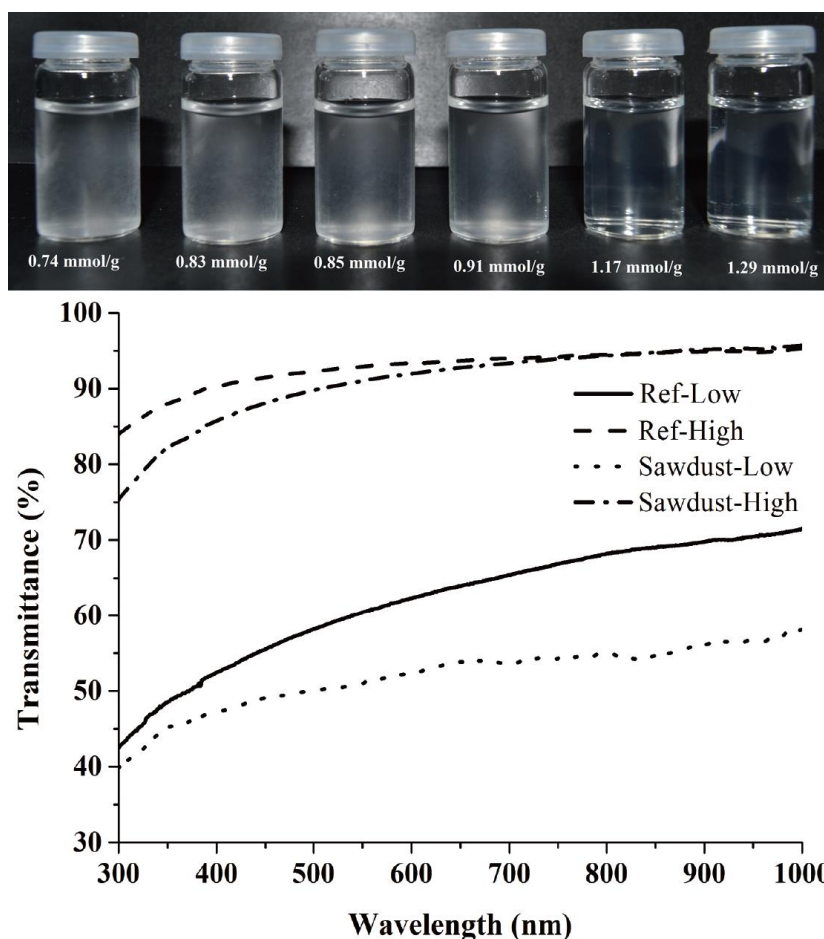


Figure 6. Photographs of the sawdust CNF suspensions (0.1%) with different charge densities and the UV-Vis transmittance spectra of the CNF suspensions (0.1%) prepared from reference bleached kraft pulp (Ref BKP-Low/-high charge) and sawdust pulp (Sawdust-Low/-High charge). Adapted with permission from *Paper II*, Copyright (2014) Springer.

As shown in **Figure 7**, the TEM image of the CNFs prepared from reference BKP shows similar geometric sizes as in literature (Jonoobi et al., 2015), i.e. 5-10 nm in width and 200-600 nm in length. However, TEM images of CNFs that was prepared from sawdust fiber, especially the one with low charge density (Sawdust-Low charge), show slightly larger width and shorter length compared with the reference due to the short fiber of the sawdust pulp (length 0.59 mm); and the images also show partial cellulose fibrils bundles or lateral aggregates with diameter of ca. 20 nm due to a lower charge density (Saito et al., 2007).

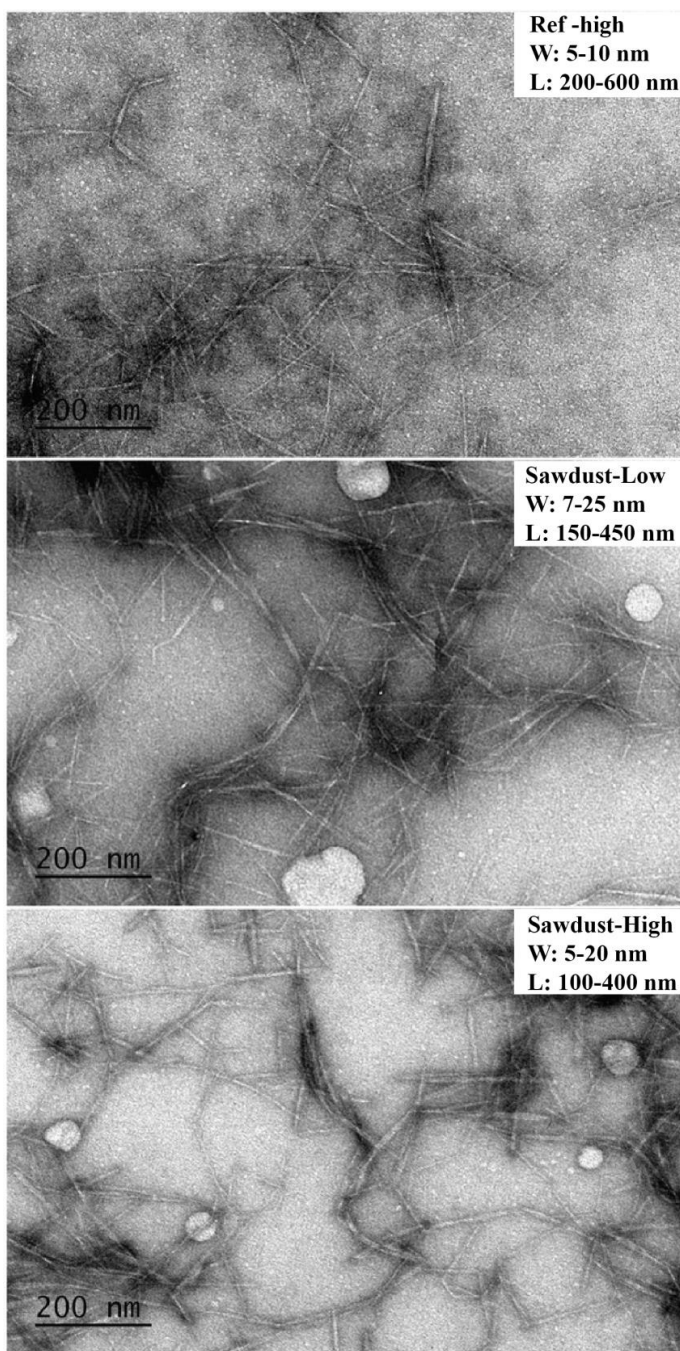


Figure 7. TEM images of the CNF suspensions with different charge densities (carboxylate content) prepared from reference bleached kraft pulp (Ref BKP-high charge) and sawdust pulp (Sawdust-Low charge and Sawdust-High charge). Adapted with permission from Paper II, Copyright (2014) Springer.

4.2.2 Mechanical properties of the sawdust CNF free-standing films

Transparent and tough sawdust CNF free-standing films were prepared by vacuum filtration, and they were found to have comparable or even better mechanical properties (**Table 1**) than the reference BKP CNF films.

Therefore, the preparation of CNF suspension and its films suggests a potential route to upgrade sawdust “waste” into valuable products. For example, the CNFs and its film may find applications as transparent and biodegradable materials; as pharmaceutical excipient; as food additives such as rheology modifier; and as reinforcement additives in composite materials manufacture (Aspler et al., 2013).

Table 1. TEMPO-mediated oxidation conditions of reference BKP and sawdust fibers; the charge density and degree of polymerization (DP) of CNF suspensions; and the mechanical properties of the resultant free-standing films.

Sample	NaClO (mmol/g)	Oxidation time (h)	Charge density (mmol/g)	DP	Young's modulus (GPa)	Tensile strength (MPa)
Ref. -Low	5	4.0	0.85 ± 0.03	-	6.4 ± 0.5	159.3 ± 9.3
Ref. -High	10	9.5	1.17 ± 0.06	521	5.9 ± 0.5	151.2 ± 13.2
Sawdust-Low	5	6.0	0.92 ± 0.04	-	6.0 ± 0.5	161.5 ± 5.0
Sawdust-High	10	9.5	1.16 ± 0.03	467	6.4 ± 0.5	171.6 ± 9.9

4.3 CNF-based biocomposites with electroconductivity and antimicrobial activity (Paper III)

Electrically conducting polymers have attracted a lot of attention due to the broad range of potential application areas especially in electrochemical biosensing and as biomedical materials for health care diagnostics (Leleux et al., 2014). Polypyrrole (PPy) is one of the most studied conducting polymers possessing interesting properties, such as biocompatibility and tunable electrical conductivity (Ramanaviciene et al., 2007). However, the poor processability owing to the insolubility and infusibility of the conducting polymers limits their use in practical applications (Skotheim & Reynolds, 2007). To overcome this problem, CNFs possessing high mechanical stiffness can be used as a reinforcement additive or as a template for polymer processing (Leppänen et al., 2013). The scheme in **Figure 8** illustrates the preparation of CNF-PPy biocomposites, in which the CNFs were used as a template for PPy coating during polymerization (oxidation), and the silver nanoparticles were incorporated to improve the electrical conductivity of the biocomposites and also to offer the antimicrobial properties.

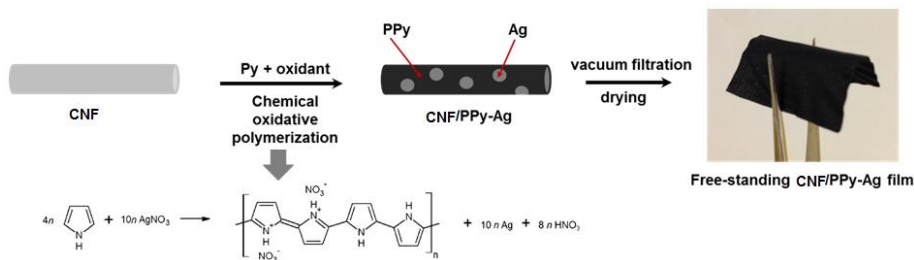


Figure 8. Scheme for the preparation of CNF-PPy biocomposites. Adapted with permission from Paper III, Copyright (2014) American Chemical Society.

4.3.1 FTIR spectra of the CNF-PPy biocomposites

FTIR spectra of the CNFs, and CNF-PPy biocomposites with different silver content were recorded and shown in **Figure 9** to study the structural changes occurring during the biocomposites preparation.

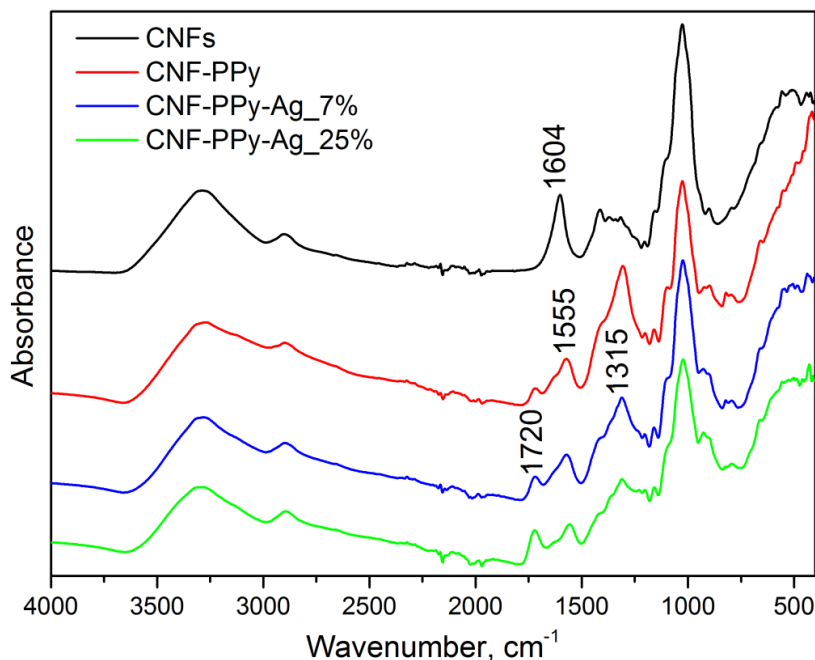


Figure 9. FTIR spectra of CNF films, CNF-PPy biocomposites, and CNF-PPy-Ag biocomposites with different silver weight percentages. Adapted with permission from Paper III, Copyright (2014) American Chemical Society.

The characteristic bands at 1604 cm^{-1} in the CNFs, and 1720 cm^{-1} in the CNF-PPy biocomposites suggest the presence of the carboxylate groups in sodium and proton forms on the cellulose surface (Saito et al., 2011). The peak at 1555 cm^{-1} in CNF-PPy biocomposites corresponds to the C=C stretching in the PPy, while the peak at 1315 cm^{-1} attributes to the C-N bonds in PPy (Chougule et al., 2011). The

diminishing of the carboxylate group peaks, and the appearance of the PPy bands in the FTIR spectra of the CNF-PPy biocomposites suggest that the PPy was coated on the surface of the CNFs.

4.3.2 Morphology and topography of the CNF-PPy biocomposites

The surface morphology and the nanoscale topography of the CNF-PPy biocomposites were studied by SEM and AFM imaging, as shown in **Figure 10** and **Figure 11**, respectively. The SEM and AFM images of the pure CNF film showed a rather smooth surface with a lower root mean square (RMS) roughness (**Figure 11**). After coating with PPy and incorporation of silver nanoparticles, the surface heterogeneity and RMS roughness further increased. Aggregation and accumulation of silver particles with diameters from a few nanometers to dozens of micrometers on the films surface are visible in the SEM images (**Figure 10**) with increasing of the silver concentration in the biocomposites.

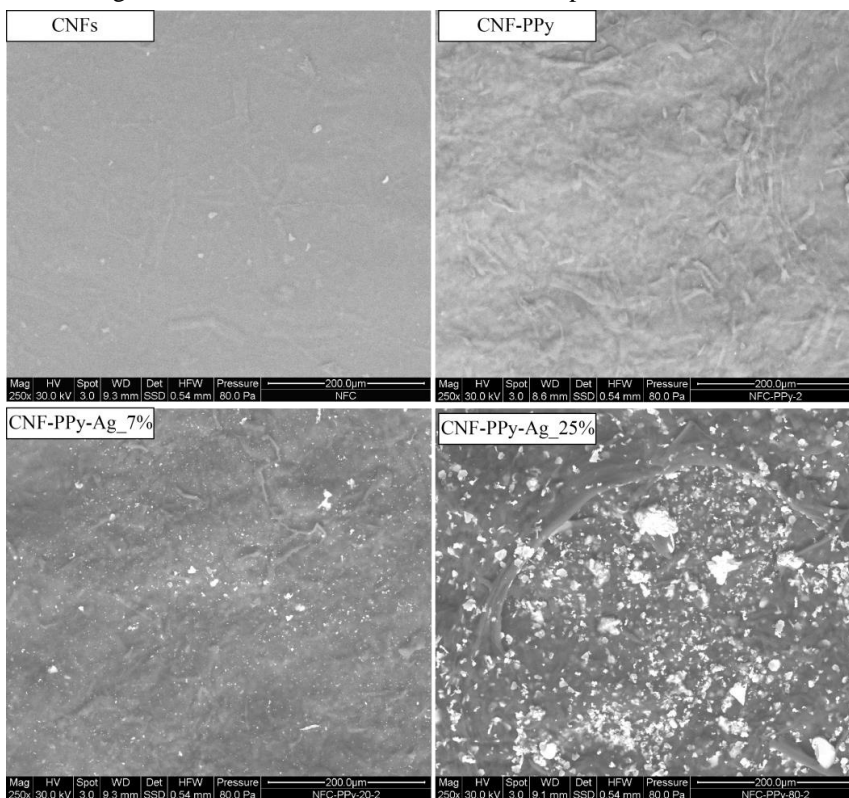


Figure 10. SEM images of CNF films, CNF-PPy biocomposites, and CNF-PPy-Ag biocomposites with different silver weight percentages.

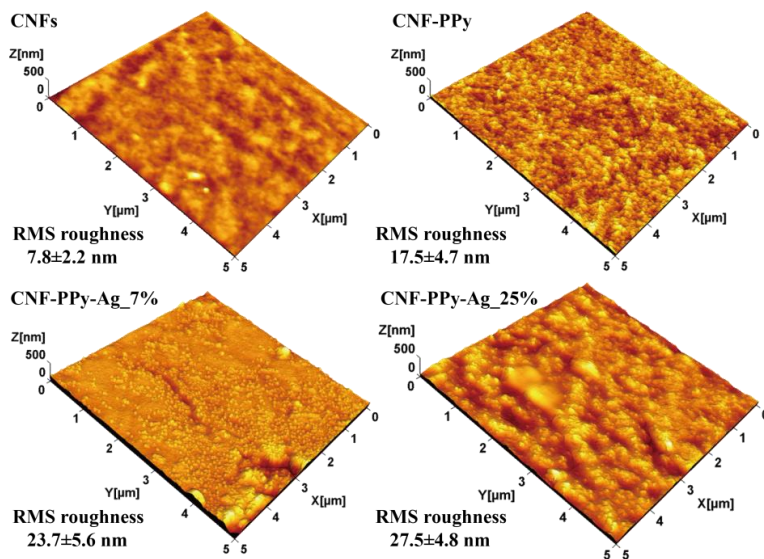


Figure 11. AFM topographical images of CNF films, CNF-PPy biocomposites, and CNF-PPy-Ag biocomposites with different silver weight percentages. Adapted with permission from Paper III, Copyright (2014) American Chemical Society.

4.3.3 Mechanical, electrical conductive, and antimicrobial properties of CNF-PPy biocomposites

To overcome the poor processability of the electrical conducting polymers, such as the PPy in this case, the CNFs, which have excellent mechanical strength, were used to reinforce the biocomposites (Skotheim & Reynolds, 2007). The mechanical strength of the CNF-PPy biocomposites is shown in **Table 2**, and the representative stress-strain curves are shown in **Figure 12**. The coating of the CNFs with PPy, and incorporation of silver nanoparticles decreased the tensile strength and Young's modulus of the materials. The in-situ polymerization of PPy on the CNF surface, and the aggregation of the silver particles resulted in a heterogeneous film structure, which hindered the interfibrillar interaction, and consequently decreased the mechanical strength of the films. However, these strength values are still sufficiently high for preparing free-standing CNF-PPy biocomposite films.

The antimicrobial properties of the CNF-PPy biocomposites were tested on yeast (*C. albicans*), a Gram-negative bacterium (*S. infantis*), and two Gram-positive bacteria (*C. albicans*, and *S. aureus*) (**Table 2**). The antimicrobial activity against the yeast and bacteria was characterized by measuring the growth inhibition zones around the sample edges. As shown in **Table 2**, the coating of the CNFs with PPy introduced not only the electrical conductivity, but also the antimicrobial activity against *L. monocytogenes*. Incorporation of silver nanoparticles further enhanced the antimicrobial activity, and also offers biocomposites with border antimicrobial activity against the *S. aureus*. These antimicrobial effects of the CNF-PPy

biocomposites make the materials potential candidates for biomedical application, such as wound healing.

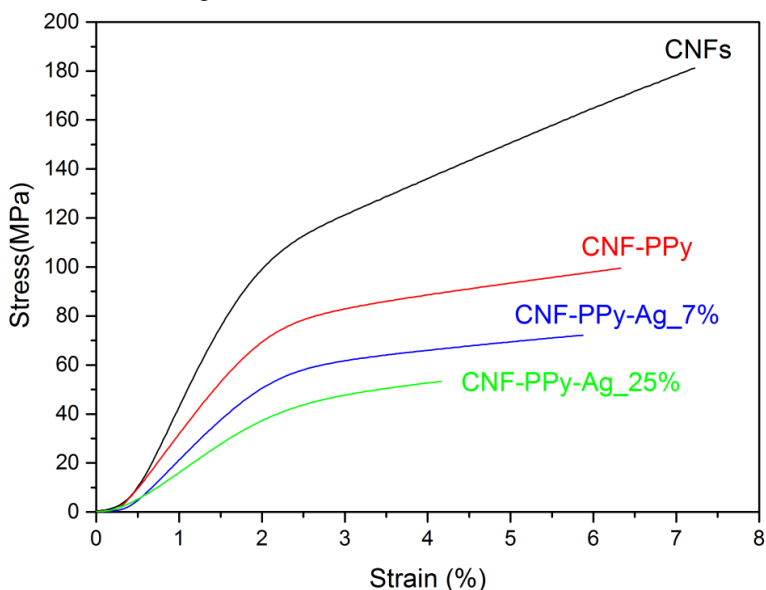


Figure 12. Selected representative stress-strain curves of CNF films, CNF-PPy biocomposites, and CNF-PPy-Ag biocomposites with different silver weight percentages. Adapted with permission from Paper III, Copyright (2014) American Chemical Society.

Table 2. The electrical conductivity, mechanical strength, and antimicrobial effects of CNF-PPy biocomposites. Adapted with permission from Paper III, Copyright (2014) American Chemical Society.

Sample	Young's modulus (GPa)	Tensile strength (MPa)	σ (S/cm)	<i>C. albicans</i>	<i>L. monocytogenes</i>	<i>S. aureus</i>	<i>S. infantis</i>
CNFs	6.9 ± 0.6	182.9 ± 12.4	$<10^{-6}$	- ^a	-	-	-
CNF-PPy	4.3 ± 0.4	90.7 ± 7.7	2×10^{-3}	-	±	-	-
CNF-PPy-Ag_7%	3.1 ± 0.5	68.7 ± 3.9	3×10^{-5}	-	+	+	-
CNF-PPy-Ag_25%	2.4 ± 0.4	51.8 ± 2.5	1×10^{-6}	-	++	+	-

^a - = no zone of inhibition around the sample;

± = a just discernible growth inhibition;

+ = a distinct zone of inhibition of ca. 2 mm around the sample;

++ = an inhibition zone of ≥ 3 mm around the sample.

4.4 CNF-based scaffolds for 3D cell culture of tumor cells (Paper IV)

Owing to the intrinsic non-toxicity, biocompatibility, and biodegradability, the CNFs and its biocomposites are increasingly studied for biomedical application, such as tissue engineering, wound healing/dressing, medical implants, and drug delivery (Jorfi & Foster, 2015). The scheme in **Figure 13** illustrates the preparation of CNF-based 3D matrices towards tissue engineering scaffold and 3D cell culture study. To mimic the cell attachment and proliferation in the 3D extracellular matrix (ECM) scaffold *in vivo* for potential 3D cell culture application, this work proposed a novel approach to encapsulate and distribute the cells in the formed CNF-based matrices, and the encapsulated cells are supposed to grow and proliferate in the CNF 3D network as *in vivo*. The structural and mechanical properties of the matrices are tuned by judiciously controlling the intrinsic properties of the CNFs (charge density and aspect ratio) and the material processing parameters (swelling media conditions and film processing techniques) to meet the requirements for potential 3D cell culture and 3D scaffold construction in tissue engineering.

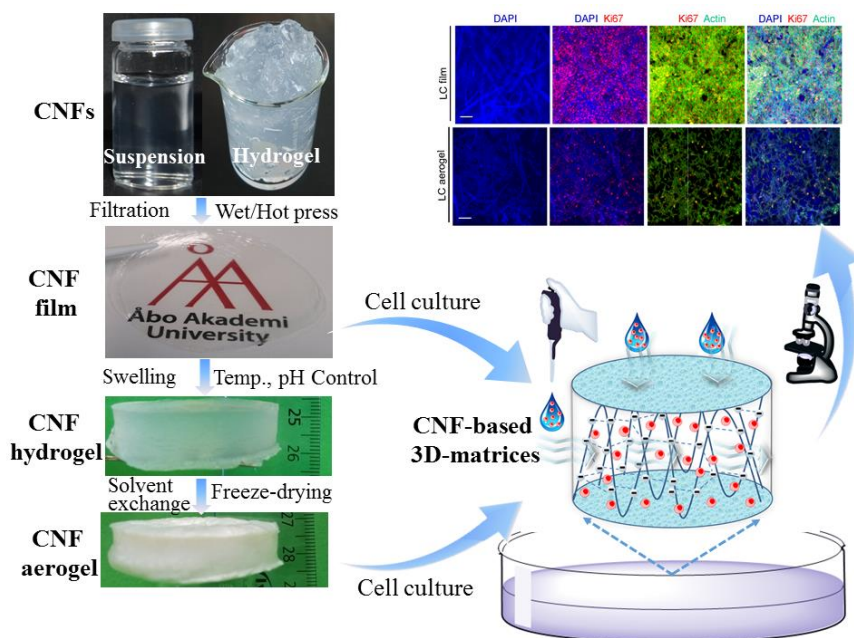


Figure 13. Scheme for the preparation of CNF-based matrices for 3D cell culture.

4.4.1 Swelling behavior of the CNF films

Water retention capacity of the scaffolds represents its ability to maintain extracellular homeostasis (Frantz et al., 2010). Different approaches to control the swelling degree of the CNF-based scaffold, i.e. by controlling the swelling time, the temperature and pH of the swelling media, and the film press methods (wet press or hot press), are shown in **Figure 14**. The HC CNF films showed faster (**Figure 14A**, higher slope of the HC CNF curve before 10.0 h) and higher maximal

swelling ability (**Figure 14B**) than those of the LC ones due to the higher electrostatic repulsion forces, which contribute to the construction of the CNF hydrogel 3D networks (Rimmer, 2011b). Change of the pH of the swelling media results in the dissociation or association of the carboxylic acid group (pK_a 3.0-5.0) (Junka et al., 2013; Spaic et al., 2014) and consequently changes the electrostatic repulsion, which is the key to tune the swelling of the hydrogel scaffold. Hot press treatment is a rapid method to prepare the CNF free-standing films (Österberg et al., 2013), which however causes lower swelling degree of the scaffolds compared to the wet press treatment due to the irreversible hornification effect at high drying temperature (80 °C) (Liu et al., 2012).

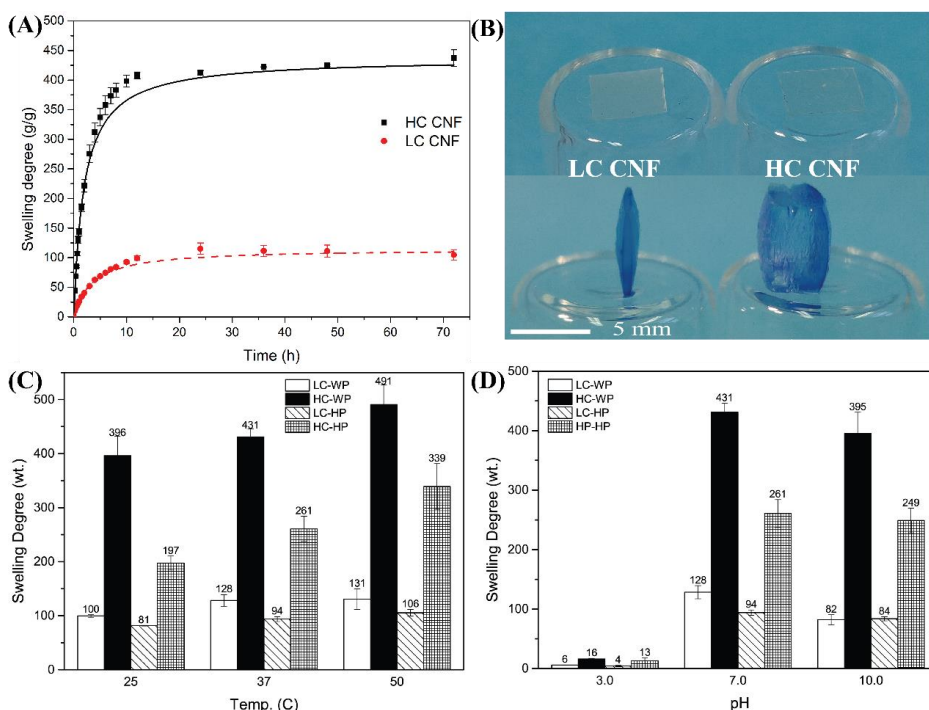


Figure 14. Tuning the swelling degree of the CNF films by controlling the CNF charge density, the swelling time (A), temperature (C), and pH (D) of the swelling media, and the film pressing methods (wet press (WP), or hot press (HP)). (B) Pictures of the CNF films before and after swelling in water (stained with methylene blue). Adapted and modified from paper IV, Copyright (2016), Elsevier.

The tunable swelling capacity of a CNF matrix by judicious control of the material intrinsic properties and processing approaches can potentially be used to load them with pharmaceutical compounds or biomolecules like proteins, bioactive polysaccharides, or cells for biomedical and pharmaceutical applications (Rimmer, 2011b). In this work, the tumor cells (Hela and Jurkat cells) were supposed to be sucked into the networks of the hydrogels during swelling, meanwhile the cells

distribute and grow in the CNF scaffold as in the ECM *in vivo*. More importantly, the CNF films with desired swelling capacity enables the efficient preservation of a moist environment that resembles the highly hydrated state of the native tissue *in vivo* (Cushing & Anseth, 2007; Cutting, 2003; Rimmer, 2011a; Winter, 1962).

4.4.2 Porous structure and mechanical properties of the CNF scaffolds

ECM-mimicking scaffolds should have appropriate pore parameters for cell penetration, cell migration, cellular ingrowth, nutrients transportation, and removal of metabolic waste (Stella et al., 2010); furthermore, scaffolds should also provide sufficient mechanical integrity to withstand the dynamic environment upon tissue engineering applications.

Figure 15 shows the porous structure of the CNF scaffold, which has open pores with 10-100 μm in diameters and fine networks in nanometer scale, suggesting they are applicable for most human cells to grow into (Utah, 2016). As shown in **Table 3**, the specific surface area (SSA) and mechanical properties of the scaffolds can also be tuned using the CNFs with appropriate chemical (charge density) and physical (aspect ratio) properties, and by controlling the processing parameters without introducing any toxic chemicals. Generally, the HC CNF-based aerogel scaffolds have higher SSA values but lower mechanical strength than those of the LC CNF-based ones; and all parameters (swelling temperature, pH, wet/hot press) that can result in high swelling degree of the hydrogel will lead to a low mechanical strength and high SSA value (aerogels). The mechanical strength of the CNF-based scaffolds (with modulus in 3-100 kPa) can cover the stiffness requirement of the tissue from the soft liver to the tough cartilage (Janmey & Miller, 2011), suggesting the potential for different tissue engineering applications.

Table 3. Mechanical properties of the CNF hydrogels and aerogels; and the specific surface area (SSA) of the CNF aerogels. Adapted with permission from paper IV, Copyright (2016), Elsevier.

	Sample	Compressive Stress (kPa)	Modulus (kPa)	SSA (m ² /g)
Hydrogel	HC-WP-25 ^a	4.1 ± 0.5	9.6 ± 1.3	-
	HC-WP-50	1.1 ± 0.2	3.0 ± 0.4	-
	HC-WP-25 (pH3) ^b	11.1 ± 3.8	35.5 ± 6.7	-
	HC-HP-25	4.4 ± 0.2	10.8 ± 0.8	-
	LC-WP-25	7.5 ± 0.4	27.6 ± 4.1	-
	LC-WP-50	5.2 ± 0.6	23.1 ± 2.10	-
	LC-WP-25 (pH3) ^b	16.0 ± 0.9	33.3 ± 6.7	-
	LC-HP-25	10.4 ± 1.0	30.6 ± 5.9	-
Aerogel	HC-WP-25	28.0 ± 6.6	24.7 ± 0.7	308.0
	HC-WP-50	34.2 ± 3.1	28.5 ± 3.4	297.6
	HC-WP-25 (pH3) ^b	35.7 ± 5.4	47.2 ± 3.6	279.4
	HC-HP-25	31.8 ± 4.9	26.5 ± 1.5	267.4
	LC-WP-25 ^c	60.3 ± 5.9	65.5 ± 3.5	242.1
	LC-WP-50 ^c	94.4 ± 14.9	100.0 ± 6.2	203.6
	LC-WP-25 (pH3) ^{b,c}	104.41 ± 2.76	88.1 ± 5.5	157.5
	LC-HP-25 ^c	62.80 ± 5.10	66.9 ± 4.0	175.9

^a The samples were named sequentially according to the charge density of the CNFs (low charge and high charge, LC and HC); the CNF film press processing approaches (wet press and hot press, WP and HP); the temperature (25, 37, 50 °C) and pH value (3.0, 7.0, 10.0) of the swelling media.

^b Samples swelled in media with a pH of 3.0. If not specified, other samples swelled in a neutral environment.

^c Values were obtained from the measurement of two overlapped specimens to reach the thickness limit (ca. > 1.0 mm) of the DMA measurement. If not specified, other samples were determined individually.

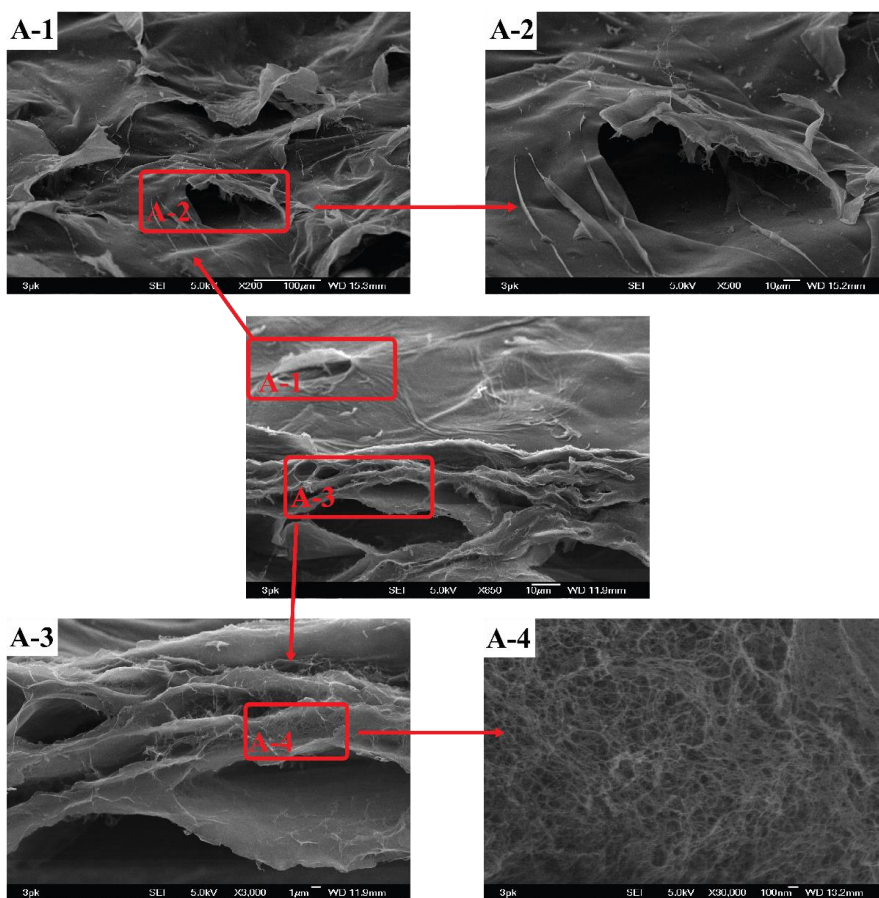


Figure 15. Representative SEM images of the CNF aerogel (medium charge density, wet pressed, swelled in neutral media at r.t.). Adapted with permission from paper IV, Copyright (2016), Elsevier.

4.4.3 Cell viability and proliferation in the CNF-based scaffolds

To mimic the ECM scaffolds for 3D cell culture and for tissue engineering application, the biocompatibility and efficacy of the CNF-based matrices were assessed (Neves et al., 2015).

Two cell models, the epithelial-derived HeLa cells and hematopoietic-derived Jurkat cells, widely used for tumor studies, were applied to assess the biocompatibility of the CNF-based matrices (films of HC-WP and LC-WP; aerogels of HC-WP-25 and LC-WP-25). The cell viability and proliferation in the CNF matrices, and the related confocal images are depicted in **Figure 16** and **Figure 17**, respectively.

The non-toxicity of the CNF-based matrix towards HeLa cells and Jurkat cells was confirmed by the results that both the CNF films and aerogels could support the

survival of HeLa cells and Jurkat cells, and no clear cell toxicity was observed with less than 5% cell death in all settings (**Figure 16A**). Interestingly, the CNF films, especially the LC CNF films, had lower cell death (**Figure 16A**) and higher proliferation rate (**Figure 16C**) than the aerogels and the control glass slides (mock, **Figure 16A**). This is probably due to the lower efficiency of cell incorporation and distribution in the aerogels scaffolds when compared to the film scaffolds. In the film scaffolds, the cells were incorporated into the scaffolds with the Donnan effect and the subsequent osmotic effect during the film swelling (Alberts, 2002; Rimmer, 2011a). Moderate surface charge of the matrices has been identified to play an important role in the cell biological response and might enhance the cell growth and proliferation (Cartmell et al., 2014; Itoh et al., 2006), which has also been confirmed by the better cell viability and proliferation of the LC film matrices in this work (**Figure 16A and 16B**). However, as shown in **Figure 16A, 16B**, and **Figure 17**, a higher surface charge of the matrices may hinder the cell biological response and result in slower growth and a higher cell death rate.

The confocal imaging analysis (**Figure 17A**) also suggests that the CNF film matrices displayed a striking induction in proliferating cells into the 3D matrices, as indicated by the intense distribution of cells proliferation marker, nuclear antigen ki67, as well as cytoskeleton marker actin. The ki67 and actin positive cell population in aerogels were much smaller (**Figure 17B**), supporting the proliferation data in **Figure 16C**. This observation further demonstrates that cells growing in CNF film matrices had increased cell proliferation activity.

The CNF-based matrices (film, hydrogel, and aerogel) with biocompatibility, permeability, reasonable mechanical and chemical stability, and tunable morphology and structure are very promising candidates for 3D cell culture study and tissue engineering applications.

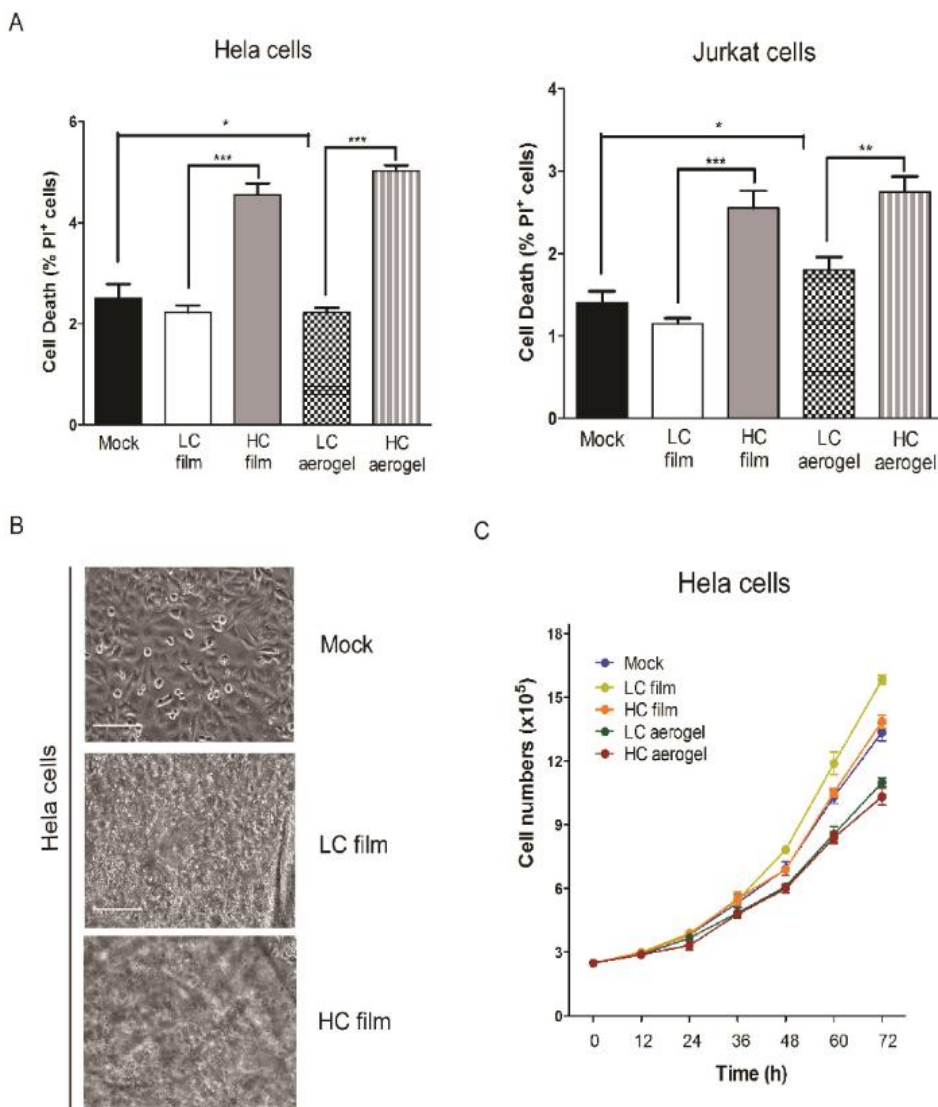


Figure 16. (A) Cell death rate of *Hela* cells and *Jurkat* cells in the CNF matrices and control glass slides (Mock) after 72 h incubation. \pm s.e.m.; $n=4$. *, $p<0.05$; **, $p<0.01$; ***, $p<0.001$. (B-C) Representative phase contrast images and growth curves of *Hela* cell lines after incubation in the CNF matrices for 72 h. \pm s.e.m.; $n=3$. Scale bar, 50 μ m. Wet pressed high and low charge CNF films (HC-WP and LC-WP), and their resultant aerogels (HC-WP-25 and LC-WP-25) were used for testing. Adapted with permission from paper IV, Copyright (2016), Elsevier.

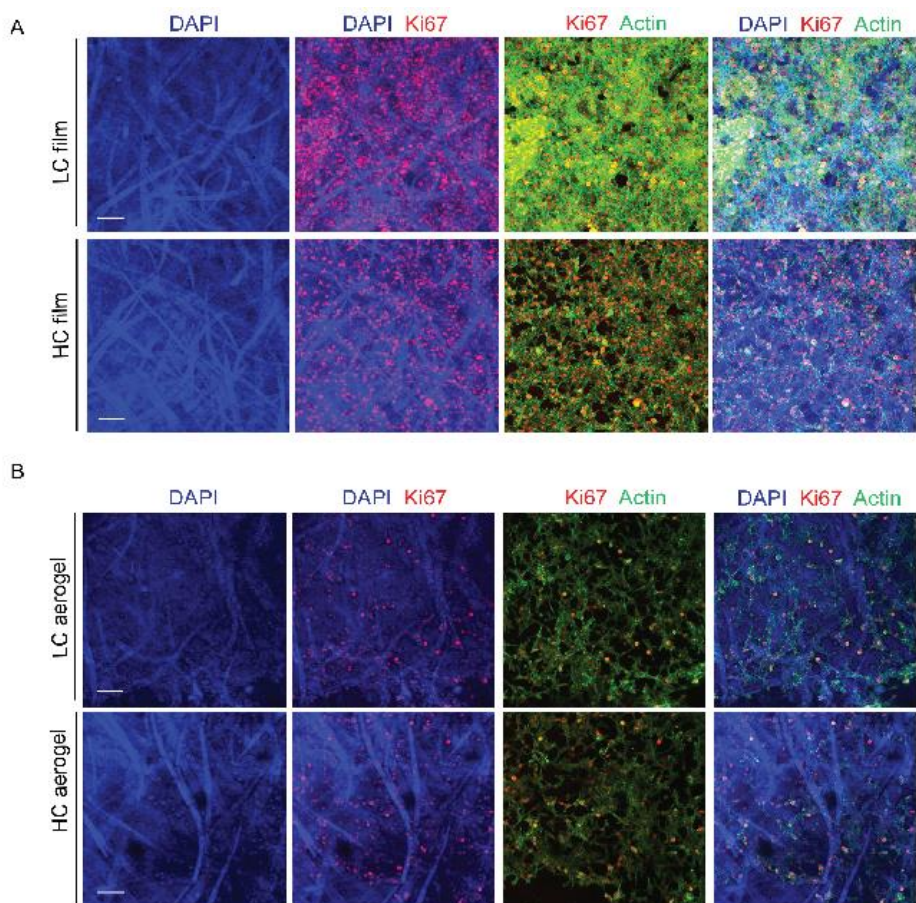


Figure 17. Representative confocal images of the expression of Ki67 (in red) and cytoskeleton marker actin (in green) in Hela cells growing into HC and LC films (A) and aerogels (B) after 72 h incubation. Matrices and nucleus were counterstained with DAPI (blue). Scale bar, 200 μm . Adapted with permission from paper IV, Copyright (2016), Elsevier.

4.5 All-polysaccharide composite scaffolds for potential wound healing application (Paper V)

Polysaccharides have increasingly found application as promising materials for biomedical and pharmaceutical devices, e.g. as biocompatible hydrogels or scaffolds in tissue engineering, as artificial skin for wound healing, and as biodegradable carrier for drug delivery (Popa, 2011). Modern wound care and tissue engineering have emerged from the use of biocomposites to create a temporary wound care system on the wound surfaces, or to replace damaged or diseased tissues in the form of three-dimensional (3D) matrices (Czaja et al., 2007; Moroni et al., 2006). The mechanical and structural properties of a scaffold in biomedical application are believed to play crucial roles in the cellular behavior,

e.g. cell proliferation, gene expression, maintenance of phenotype, and biosynthetic activity in tissue engineering (Lin et al., 2011a); and therefore the goal of this work was to tune the mechanical and structural properties of CNF-based all-polysaccharide composite hydrogels, and to investigate how the biocompatibility of the composite hydrogels is influenced by the mechanical and structural properties of the scaffolds.

Inspired from the mechanical integrity of plant cell walls, in which the cellulose and hemicelluloses are closely associated (Eckardt, 2008; Johansson et al., 2004; Park & Cosgrove, 2015), hemicelluloses are supposed to adsorb on the nanocellulose surface to reinforce the mechanical properties of the nanocellulose hydrogel. As depicted in **Figure 18**, different hemicelluloses with various ratios were incorporated into the CNF hydrogel network in two approaches to tune the microscopic and mechanical properties of the composite hydrogels, thus making it possible to control properties that are important for biomedical applications like wound healing and tissue engineering (Bonilla et al., 2015; Prakobna et al., 2015a; Prakobna et al., 2015b; Stevanic et al., 2014).

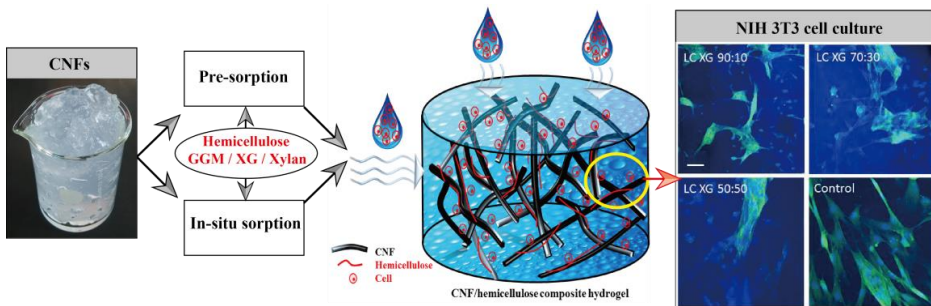


Figure 18. Scheme for the preparation of all-polysaccharide composite hydrogel for potential wound healing application.

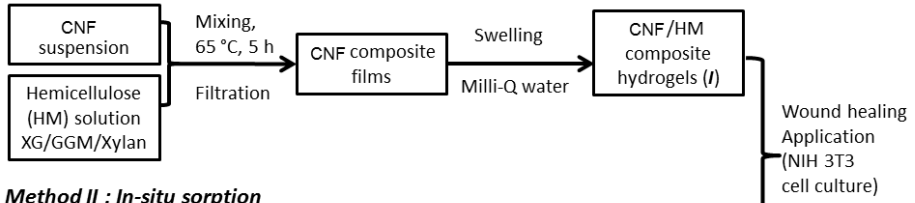
4.5.1 Incorporation of hemicelluloses into the CNF network and its effect on the swelling property of the composite scaffolds

Cellulose and hemicelluloses are closely associated in the plant cell wall to contribute to the rigidity of the cellulose framework in nature (Eckardt, 2008; Johansson et al., 2004; Park & Cosgrove, 2015). In this work, hemicelluloses (XG, GGM, and xylans) were incorporated into the CNF networks via pre-sorption and in-situ sorption methods as shown in **Figure 19**.

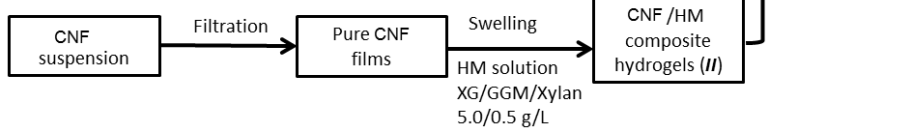
The adsorbed amount of hemicellulose was controlled by changing the hemicellulose to CNF mass ratio (pre-sorption) or by changing the hemicellulose concentration (in-situ sorption). As shown in **Figure 20A** and **Figure 20B**, all HC-CNF hydrogels had higher hemicellulose sorption capacity than those of LC-CNF due to their higher water/solution uptake capacity (**Figure 20C** and **Figure 20D**). The XG showed the highest sorption capacity to the nanocellulose, especially the HC-CNF, by both sorption approaches, followed by GGM and xylan. This is due

to the fact that the hemicelluloses adsorption capacity was affected by the structural complexity difference of the hemicelluloses more than just by the molar mass (Eronen et al., 2011). The high and tunable affinity of hemicelluloses to cellulose opens the opportunity for surface modification of the nanocellulose and to tailor the mechanical properties of the composite materials (Bodin et al., 2007; Bonilla et al., 2015; Stevanic et al., 2014).

Method I : Pre-sorption



Method II : In-situ sorption



Wound healing Application (NIH 3T3 cell culture)

Figure 19. Preparation of all-polysaccharide composite hydrogels by incorporation of different hemicelluloses in the CNF networks with two methods. Adapted with permission from paper V, Copyright (2016), Springer.

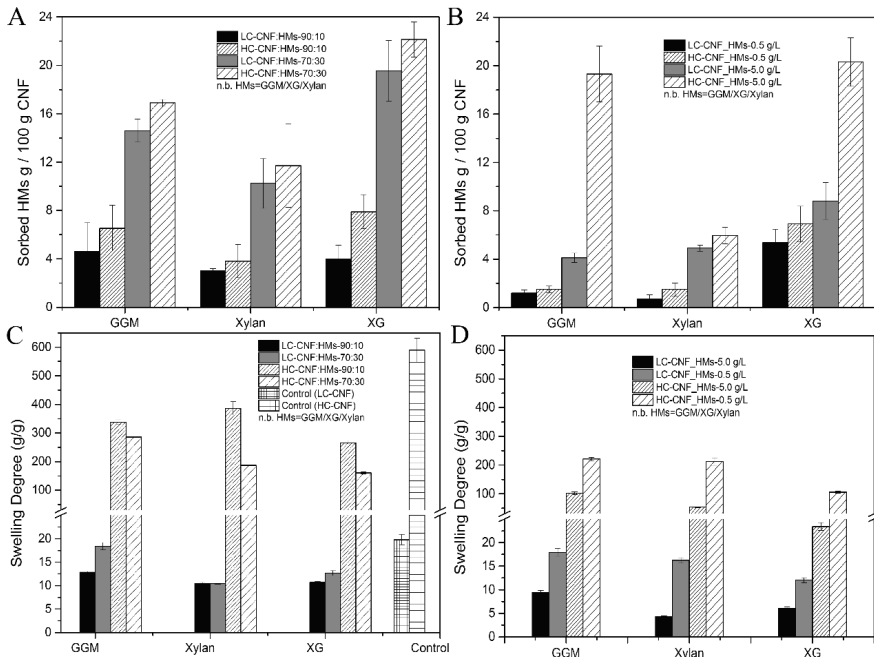


Figure 20. The amount of hemicelluloses incorporated into the CNF matrices by pre-sorption (A) and in-situ sorption (B). Maximal swelling degree of composite films in pure water (C) and of the pure CNF films (D) in hemicellulose solutions with different concentrations (5.0 g/L and 0.5 g/L). The control refers to the

maximal swelling degree of the pure CNF films in pure water. Adapted with permission from paper V, Copyright (2016), Springer.

4.5.2 Morphological properties of the all-polysaccharide composite scaffolds

The representative porous structure of the CNF XG composite scaffolds is shown in **Figure 21**. The HC-CNF containing aerogels show more and larger open pores than those of LC-CNF due to the higher swelling degrees during hydrogel formation (**Figure 20C and 20D**). The in-situ sorbed hemicelluloses were found to deposit on the surface and in some of the pores, probably due to the self-association and aggregation of the hemicelluloses in solutions (Eronen et al., 2011; Linder et al., 2003). However, the pre-sorbed hemicelluloses were not visible from the SEM images, and thus were supposed to tightly adsorb onto the CNFs. The pore size is estimated to be 15-50 μm for the LC-CNF composite aerogels, and 200-500 μm for the HC-CNF composite aerogels. Considering that there is 30-50% shrinkage of the aerogels during freeze-drying (Mehling et al., 2009), the pore size of the hydrogels in the wet state should fit the size requirement for fibroblast cells (average size: 16-18 μm) to penetrate into the scaffolds for growth (George & Howard, 1963).

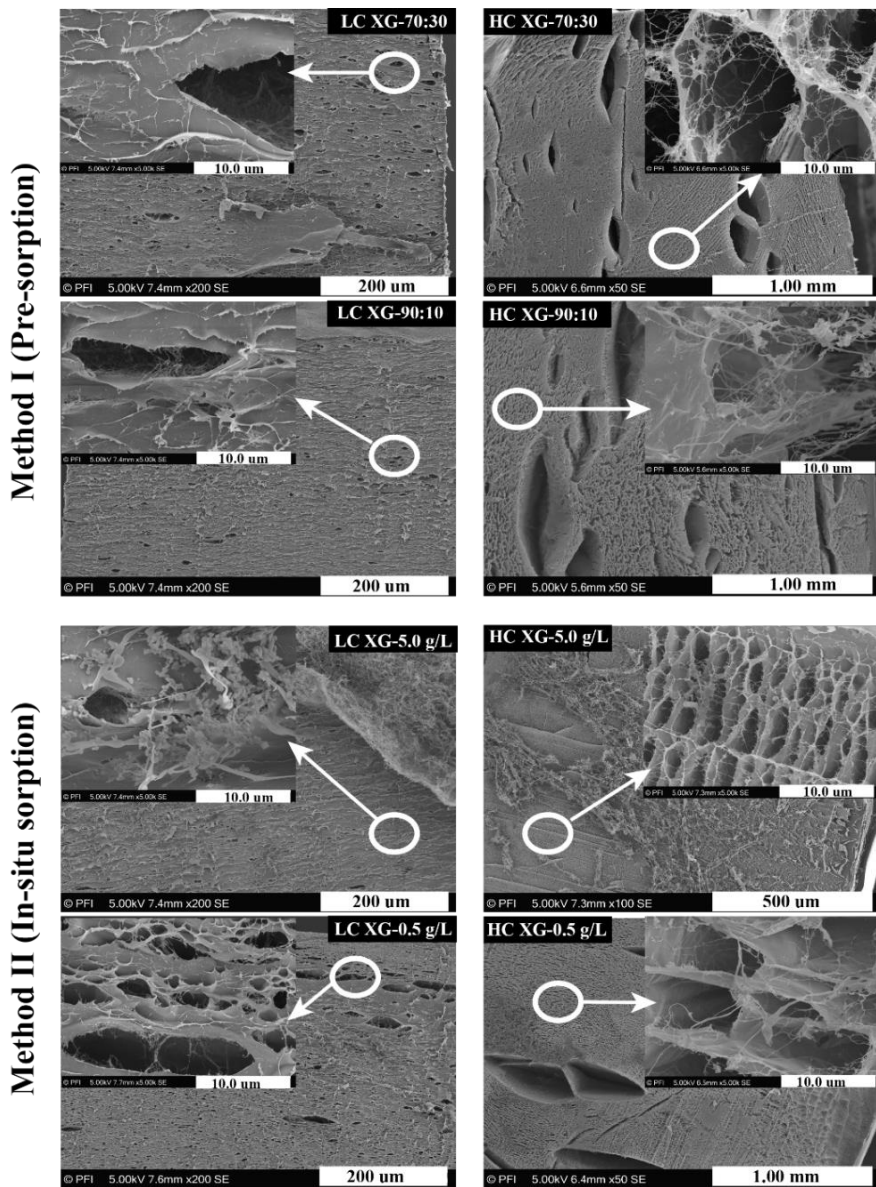


Figure 21. Representative SEM images of the CNF XG composite aerogels prepared by two different approaches and containing different amount of XG. Adapted with permission from paper V, Copyright (2016), Springer.

4.5.3 Mechanical properties of the composite scaffolds

The mechanical strength of scaffolds plays an essential role in cell adhesion, proliferation, migration, differentiation and apoptosis in biomedical applications (Muiznieks & Keeley, 2013; Syverud et al., 2015; Wells, 2013).

Table 4. Young's modulus and swelling degree of the hydrogels. Adapted with permission from paper V, Copyright (2016), Springer.

Sample	Young's modulus (kPa)	Swelling Degree (g/g)
HC-CNF-0.5 h *	60.1 ± 3.7	85.1 ± 6.3
HC-CNF-1.0 h	39.3 ± 3.9	143.2 ± 6.2
HC-CNF-3.0 h	26.0 ± 2.8	275.4 ± 14.8
HC-CNF-5.0 h	21.1 ± 3.4	337.3 ± 14.5
HC-CNF-7.0 h	19.2 ± 1.7	373.2 ± 13.8
HC-CNF-9.0 h	16.4 ± 2.0	390.5 ± 11.0
HC-CNF-12.0 h	14.9 ± 1.5	407.8 ± 5.9
HC-CNF-24.0 h	-	583.3 ± 58
LC-CNF-24.0 h	19.4 ± 4.0	17.8 ± 1.0
HC-CNF:XG_70:30	26.1 ± 3.4	160.4 ± 3.58
HC-CNF:XG_90:10	20.0 ± 2.9	265.9 ± 7.3
HC-CNF:GGM_70:30	11.8 ± 1.8	285.8 ± 0.6
HC-CNF:GGM_90:10	9.8 ± 1.6	338.4 ± 9.1
HC-CNF:Xylan_70:30	19.2 ± 3.4	186.6 ± 14.2
HC-CNF:Xylan_90:10	10.0 ± 1.1	385.9 ± 23.3
LC-CNF:XG_70:30	107.8 ± 5.5	12.7 ± 0.5
LC-CNF:XG_90:10	81.4 ± 6.2	10.7 ± 0.2
LC-CNF:GGM_70:30	60.0 ± 4.9	18.4 ± 0.8
LC-CNF:GGM_90:10	40.7 ± 3.4	12.8 ± 0.2
LC-CNF:Xylan_70:30	98.3 ± 7.2	10.39 ± 0.11
LC-CNF:Xylan_90:10	48.7 ± 4.2	10.48 ± 0.2
HC-CNF-XG_5	51.9 ± 1.6	23.43 ± 0.8
HC-CNF-XG_0.5	31.7 ± 2.9	105.55 ± 3.0
HC-CNF-GGM_5	21.9 ± 2.8	102.5 ± 4.6
HC-CNF-GGM_0.5	19.6 ± 3.5	221.1 ± 5.6
HC-CNF-Xylan_5	17.0 ± 1.7	53.3 ± 1.4
HC-CNF-Xylan_0.5	13.3 ± 2.7	212.0 ± 13.4
LC-CNF-XG_5	-	6.1 ± 0.3
LC-CNF-XG_0.5	47.6 ± 3.2	12.1 ± 0.5
LC-CNF-GGM_5	41.2 ± 2.3	9.4 ± 0.4
LC-CNF-GGM_0.5	31.0 ± 3.7	17.9 ± 0.8
LC-CNF-Xylan_5	57.7 ± 2.7	4.3 ± 0.1
LC-CNF-Xylan_0.5	31.9 ± 4.2	16.2 ± 0.6

* HC-CNF hydrogels prepared by swelling under different time. LC-CNF was not selected due to the significantly lower swelling degree (max. ca. 18 g/g).

As shown in **Table 4**, the overall Young's moduli of the pure CNF hydrogels and the composite hydrogels are in the range of 10-100 kPa, which can cover the mechanical stiffness requirement of muscle tissue (Janmey & Miller, 2011). The swelling degree of the hydrogel was reported to significantly affect its mechanical

behavior (Barbucci, 2009; Okay, 2010). As shown in **Table 4**, the Young's moduli of the pure HC-CNF hydrogels and HC-CNF composite hydrogels were found to negatively correlate with the corresponding swelling degree due to the plasticizing effect of water in the hydrogel (Okay, 2010; Sehaqui et al., 2011; Yang et al., 2013). The XG-CNF composite hydrogels showed the highest mechanical strength compared with those of GGM and xylan when other conditions were the same (e.g. CNF charge density, CNF-hemicellulose ratio, and hemicellulose concentration). This might be due to the fact that the highly branched XG was adsorbed and cross-linked with cellulose fibers, which resulted in a higher crosslinking density and thus lower swelling degree of the scaffolds (Bonilla et al., 2015; Lopez-Sanchez et al., 2015). Therefore, controlling of the swelling degree of the hydrogels by changing the swelling time and the incorporated hemicellulose type and amount enable tuning the mechanical properties of scaffolds, and thus allows the design of biomaterials with desired stiffness to meet the required mechanical properties in different biomedical applications (Syverud et al., 2015).

4.5.4 CNF composite scaffolds supporting 3T3 fibroblast proliferation

Supporting the survival and proliferation of the 3T3 fibroblast cells in a scaffold is the prerequisite for potential wound healing application. The proliferation of the cells in the CNF composite hydrogels was assessed to evaluate the efficacy of the scaffolds, and the results are shown in **Figure 22**. The 3T3 fibroblast cells rarely grew in the HC-CNF composite scaffolds, thus the data are not included in **Figure 22**. The higher surface charge density and the lower mechanical strength of the HC CNF-based composite hydrogel could be the reason for not supporting the survival of the cells (Cartmell et al., 2014; Itoh et al., 2006; Plant et al., 2009; Saddiq et al., 2009; Wells, 2008).

The LC-CNF composite hydrogels that were prepared by the *in-situ* sorption approach inhibited cell proliferation to a certain level regardless of their mechanical strength (**Figure 22A**), probably due to the self-aggregation and deposition of the hemicelluloses on the surface of the cellulose nanofibrils, which limited the adhesion of the cells onto the scaffolds. The inhibition effect of the *in-situ* sorbed hemicelluloses on the cellular activities may also be a result of the residual lignin in the hemicelluloses, especially the GGM and xylan (Andrijevic et al., 2008; Chinga-Carrasco & Syverud, 2014; Fukuzumi et al., 2009; Goldschmid, 1954; Sorimachi et al., 1992).

In comparison to the composite hydrogels formed by the *in-situ* sorption approach, the LC-CNF composite hydrogels that were prepared by pre-sorption of all three hemicelluloses with different ratios, especially the hydrogel incorporated with xyloglucan, promoted the cell proliferation better than the LC-CNF alone. The composite hydrogels prepared by the pre-sorption approach had higher mechanical strength than those prepared by the *in-situ* approach (**Figure 22A**). This finding

indicates the beneficial effect of the pre-sorbed hemicellulose in facilitating 3T3 cell survival, proliferation, and movement (indicated by lamellipodia formation) and probably contributed by their relatively high mechanical strength.

Moreover, the composite hydrogels containing xyloglucan had higher mechanical strength than those of other hemicelluloses with a CNF:HM ratio of 70:30. The cell culture experiment was repeated and was focused on the LC-CNF-XG composite hydrogels (pre-adsorption method), and a larger amount of XG (50:50) was also incorporated into the LC-XG composite hydrogel to further investigate the effect of the XG content on the cellular activity. Interestingly, we found that the LC XG-90:10 composite hydrogel supported cell proliferation better than the 70:30 sample, whereas the 50:50 one inhibited cell proliferation (**Figure 22C-D**), suggesting an LC:XG mixing ratio-dependent effect on cell proliferation. Such ratio-dependent effect may result from the combining effect of mechanical cues of the matrix and morphology of matrix surface, which have been shown to play important roles in cell adhesion, proliferation, angiogenesis and differentiation (Plant et al., 2009; Saddiq et al., 2009; Wells, 2008). This is probably because the adsorbed xyloglucan can enhance the mechanical stiffness and thus promote the cell growth. However, too high amount of xyloglucan will smooth the surface of the scaffolds and consequently, hinder the adhesion, proliferation and movement of the fibroblast cells.

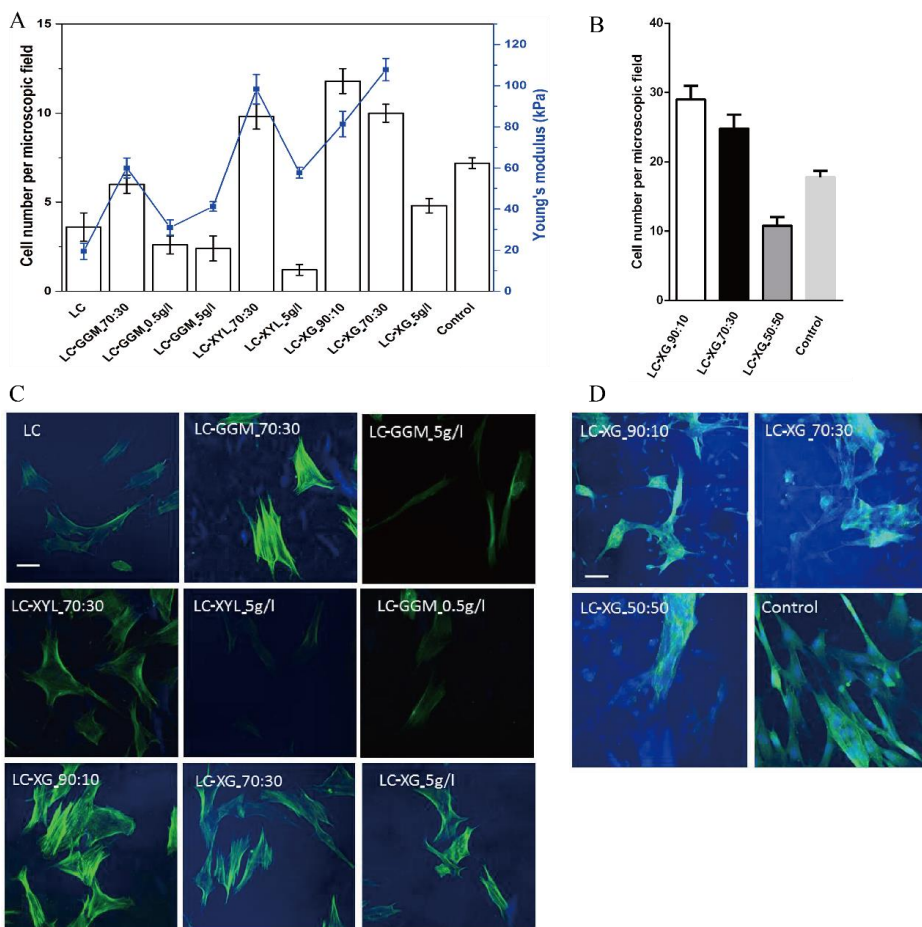


Figure 22. Proliferation of 3T3 cells in the CNF composite hydrogels (A and B) and the Young's modulus of the hydrogels (A). \pm s.e.m.; $n=5$. **, $p<0.01$; ***, $p<0.001$; 3T3 cell were incubated with the CNF matrices in a density of (A) 3×10^5 cells/24-well or (B) 5×10^5 cells /24-well for 24 hours. Representative confocal 3D images of the expression of cytoskeleton marker actin (in green) and nucleus marker DAPI (in blue) in 3T3 cells growing into the LC composite hydrogels (C and D). Scale bar, 20 μ m. Data for the HC CNF-based matrices are not shown due to the rare growth of cells on the materials. Adapted with permission from paper V, Copyright (2016), Springer.

5. Conclusion

The work of this thesis aimed at comprehensive utilization of renewable wood-derived materials, with the focus on cellulose and hemicelluloses, in the field of biomedical applications in a novel biorefinery concept. This has been done by preparation of cellulose nanofibrils (CNFs) from biomass after the hot-water extraction of hemicellulose and lignin separation; after which the CNFs was utilized as host-substrate to incorporate electrical conductive polymers, living cells, and hemicelluloses to prepare biocomposites for potential biomedical applications, such as tissue engineering and wound healing.

The CNFs and films thereof were prepared from a wood “waste”, i.e. birch sawdust, using TEMPO-mediated oxidation after hot-water extraction of hemicellulose and lignin separation. The resultant sawdust CNF free-standing films showed comparable or even better mechanical properties than those from the reference BKP at the same condition. Surface charge density (carboxylate content) and geometric morphology of the CNFs were found to play important roles in the dispersion of the CNF suspension and transmittance of light.

The CNF suspension and films thereof were explored for potential applications in advanced materials as matrices or reinforcement additives. To overcome the poor processability of conductive polymers, the CNFs were used as templates for PPy coating during polymerization, and silver nanoparticles were incorporated to improve the electrical conductivity of the biocomposites and also to offer the antimicrobial properties. Compared to pure CNFs, the polymerization of PPy and incorporation silver nanoparticles in the CNF matrix increased the surface roughness and slightly decreased the mechanical properties of the biocomposite films, but still tough enough for free-standing film applications. It is shown that the antimicrobial activity of the CNF-PPy-Ag biocomposite films inhibited the growth of Gram-positive bacteria, which correlated with the silver content in the films. The biocomposite films are therefore promising candidates for antimicrobial patches in wound healing application.

The CNFs was found to possess tangled network structure, which may found potential application in biomedical scaffolds or matrices. The highly porous CNF-based scaffolds with tunable structures were designed towards tissue engineering scaffold and 3D cell culture study. The porous structure and mechanical properties of the scaffolds can be tuned by judiciously controlling the CNF intrinsic properties (charge density and aspect ratio) and processing parameters (swelling temperature, pH, and wet and hot press treatments). The formation of the CNF-based scaffolds provided a novel approach to encapsulate and distribute the cells into the matrices. The CNF-based 3D scaffolds, especially the CNF films with low surface charge density, were found to facilitate the encapsulated Hela cells and Jurkat cells for ingrowth, survival, and proliferation.

The controllable swelling property of the CNF films opens the opportunity to incorporate biomolecules, such as polysaccharides, protein, DNA, bioactive molecules, and even living cells, into the CNF network for further biomedical application. In this work, different types of hemicelluloses were incorporated into the CNF network in two approaches (pre-sorption and in-situ sorption) with the purpose to tune the mechanical stiffness of the CNF-based composite hydrogel and their suitability for wound healing and tissue engineering. The charge density of the CNFs was found to play a key role in the hemicellulose incorporation, in the surface topography and roughness of the composite films, in the swelling of the composite hydrogels, in the mechanical strength of composite hydrogels, and in the biocompatibility of the composite hydrogel scaffolds. The mechanical properties of the composite hydrogel may have an influence on the cells viability during cell culture. The incorporated hemicelluloses showed molecular structural and dosage dependent reinforcing effects on the mechanical strength of the composite hydrogels. The XG showed the highest adsorption capacity onto the CNFs, the highest reinforcement effect, and the best biocompatibility. The pre-sorption of XG into the LC-CNF with a ratio 90:10 (CNF:XG) shows potential as scaffolds to support fibroblast cell growth and proliferation for wound healing application.

The growing demand of green and sustainable materials that are made from renewable biomass has drawn worldwide attention in the development of biorefinery. Nanocellulose production from a biomass in a novel biorefinery concept shows potential to meet this demand. Although the potential biomedical or pharmaceutical application of nanocellulose is still in its early development stages, there are already been identified and demonstrated in the lab. The challenge is to scale up and demonstrate the applicable value and to find the end-user so as to bring these new materials into the market.

6. Acknowledgements

First and foremost I would like to thank my supervisors, Stefan Willför and Chunlin Xu, for providing me the opportunity to work in the laboratory of Wood and Paper Chemistry; and for their motivation, patience, enthusiasm, and continuous support to both my research and life.

All the colleagues at the Laboratory of Wood and Paper Chemistry, at the Division of Glycoscience at KTH, and at the Paper and Fibre Research Institute are acknowledged. Especially I wish to thank Anna Sundberg, Andrey Pranovich, Annika Smeds, Leif Österholm, Jarl Hemming, Wenyang Xu, Ekaterina Korotkova, Victor Kisonen, Ann-Sofie Leppänen, Risto Korpinen, Jens Krogell, Hanna Lindqvist, Daniel Dax, Matti Häärä, Linda Nisula, Anders Strand, and Bjarne Holmbom for their assistance and valuable scientific discussion, and for all the great times spent together. Francisco Vilaplana at KTH, Kristin Syverud and Gary Chinga-Carrasco at PFI, Kirsi Mikkonen and Maija Tenkanen at the University of Helsinki, and Steven Spoljaric at Aalto University are appreciated for hosting my research exchanges and visits. I also thank all my co-authors for enjoyable collaboration.

I would like to thank all the teachers and friends at Tianjin University of Science and Technology for all the great old times. Special thanks go to Prof. Huiren Hu, and Prof. Yonghao Ni, and Prof. Qingxi Hou, for bringing me into the field of Pulping and Papermaking, biorefinery and nanocellulose world, and for their continuous support throughout my undergraduate to Ph.D. study.

All my Chinese friends in Finland, thank you all for your enthusiastic help and all the wonderful time together.

This work was carried out at the Johan Gadolin Process Chemistry Centre and Turku Centre for Biotechnology, Åbo Akademi University. Financial support from the China Scholarship Council and Graduate School of Chemical Engineering at Åbo Akademi University are acknowledged. Part of the work was carried out at the Wallenberg Wood Science Centre, and the Division of Glycoscience, KTH Royal Institute, Sweden; at the Department of Food and Environment Sciences, University of Helsinki, Finland; at the Department of Biotechnology and Chemical Technology, Aalto University, Finland; and at Paper and Fibre Research Institute and Department of Chemical Engineering, Norwegian University of Science and Technology, Norway. The NordForsk Researcher Network, the PolyRefNorth, and the Wallenberg Wood Science Center are acknowledged for funding these research exchanges and visits.

Last but not least, I would like to express my deepest gratitude to my loving family for their endless love, support, and encouragement. My dear father, mother, sister, and my beloved wife, thank you all. I love you all!

7. References

- Alberts, B. 2002. *Molecular biology of the cell*. 4th ed. Garland Science, New York.
- Alexandrescu, L., Syverud, K., Gatti, A., Chinga-Carrasco, G. 2013. Cytotoxicity tests of cellulose nanofibril-based structures. *Cellulose*, **20**(4), 1765-1775.
- Ali, F., Hongbo, Z. 2014. Recent Advances in Cellulose Nanocomposites. in: *Bio-Based Composites for High-Performance Materials*, CRC Press, pp. 167-186.
- Andrijevic, L., Radotic, K., Bogdanovic, J., Mutavdzic, D., Bogdanovic, G. 2008. Antiproliferative effect of synthetic lignin against human breast cancer and normal fetal lung cell lines. Potency of low molecular weight fractions. *Journal of B.U.ON.*, **13**(2), 241-4.
- Anirudhan, T.S., Rejeena, S.R. 2014. Aminated β -Cyclodextrin-Modified-Carboxylated Magnetic Cobalt/Nanocellulose Composite for Tumor-Targeted Gene Delivery. *Journal of Applied Chemistry*, **2014**, 1-10.
- Araki, J., Wada, M., Kuga, S. 2000. Steric Stabilization of a Cellulose Microcrystal Suspension by Poly(ethylene glycol) Grafting. *Langmuir*, **17**(1), 21-27.
- Aspler, J., Bouchard, J., Hamad, W., Berry, R., Beck, S., Drolet, F., Zou, X. 2013. Review of Nanocellulosic Products and Their Applications. in: *Biopolymer Nanocomposites*, (Eds.) D. Alain, T. Sabu, A.P. Laly, John Wiley & Sons, Inc. New Jersey pp. 461-508.
- Barbucci, R. 2009. *Hydrogels : biological properties and applications*. Springer, Milan.
- Barrett, E.P., Joyner, L.G., Halenda, P.P. 1951. The Determination of Pore Volume and Area Distributions in Porous Substances. I. Computations from Nitrogen Isotherms. *Journal of the American Chemical Society*, **73**(1), 373-380.
- Bhattacharya, M., Malinen, M.M., Lauren, P., Lou, Y.R., Kuisma, S.W., Kanninen, L., Lille, M., Corlu, A., GuGuen-Guillouzo, C., Ikkala, O., Laukkanen, A., Urtti, A., Yliperttula, M. 2012. Nanofibrillar cellulose hydrogel promotes three-dimensional liver cell culture. *Journal of Controlled Release*, **164**(3), 291-8.
- Bodin, A., Ahrenstedt, L., Fink, H., Brumer, H., Risberg, B., Gatenholm, P. 2007. Modification of nanocellulose with a xyloglucan-RGD conjugate enhances adhesion and proliferation of endothelial cells: implications for tissue engineering. *Biomacromolecules*, **8**(12), 3697-704.
- Bonilla, M.R., Lopez-Sanchez, P., Gidley, M.J., Stokes, J.R. 2015. Micromechanical Model of Biphasic Biomaterials with Internal Adhesion: Application to Nanocellulose Hydrogel Composites. *Acta Biomaterialia*, **29**:149-160
- Borrega, M., Tolonen, L.K., Bardot, F., Testova, L., Sixta, H. 2013. Potential of hot water extraction of birch wood to produce high-purity dissolving pulp after alkaline pulping. *Bioresource Technology*, **135**, 665-71.
- Brown, A.J. 1886. On an acetic ferment which forms cellulose. *Journal of the Chemical Society, Transactions*, **49**, 432.
- Brunauer, S., Emmett, P.H., Teller, E. 1938. Adsorption of Gases in Multimolecular Layers. *Journal of the American Chemical Society*, **60**(2), 309-319.
- Carletti, E., Stoppato, M., Migliaresi, C., Motta, A. 2014. The Functional Role of Extracellular Matrix. in: *Scaffolds for Tissue Engineering-Biological Design, Materials, and Fabrication*, (Eds.) M. Claudio, M. Antonella, Pan Stanford Publishing Pte. Ltd. Singapore, pp. 21-56.
- Cartmell, S.H., Thurstan, S., Gittings, J.P., Griffiths, S., Bowen, C.R., Turner, I.G. 2014. Polarization of porous hydroxyapatite scaffolds: influence on osteoblast cell proliferation and extracellular matrix production. *Journal of Biomedical Materials Research Part A*, **102**(4), 1047-52.

- Chan, B.P., Leong, K.W. 2008. Scaffolding in tissue engineering: general approaches and tissue-specific considerations. *European Spine Journal*, **17**(S4), 467-479.
- Chen, L., Zhu, J., Baez, C., Kitin, P., Elder, T.J. 2016. Highly Thermal-stable and Functional Cellulose Nanocrystals and Nanofibrils Produced Using Fully Recyclable Organic Acids. *Green Chemistry*, DOI: **10.1039/c6gc00687f**.
- Chinga-Carrasco, G., Syverud, K. 2014. Pretreatment-dependent surface chemistry of wood nanocellulose for pH-sensitive hydrogels. *Journal of Biomaterials Applications*, **29**(3), 423-32.
- Chougule, M.A., Pawar, S.G., Godse, P.R., Mulik, R.N., Sen, S., Patil, V.B. 2011. Synthesis and Characterization of Polypyrrole (PPy) Thin Films. *Soft Nanoscience Letters*, **01**(01), 6-10.
- Cushing, M.C., Anseth, K.S. 2007. Materials science. Hydrogel cell cultures. *Science*, **316**(5828), 1133-4.
- Cutting, K.F. 2003. Wound exudate: composition and functions. *Br J Community Nurs*, **8**(9 Suppl), suppl 4-9.
- Czaja, W., Romanovicz, D., Brown, R.m. 2004. Structural investigations of microbial cellulose produced in stationary and agitated culture. *Cellulose*, **11**(3/4), 403-411.
- Czaja, W.K., Young, D.J., Kawecki, M., Brown, R.M., Jr. 2007. The future prospects of microbial cellulose in biomedical applications. *Biomacromolecules*, **8**(1), 1-12.
- Dax, D., Bastidas, M.S.C., Honorato, C., Liu, J., Spoljaric, S., Seppala, J., Mendonca, R.T., Xu, C.L., Willfor, S., Sanchez, J. 2015. Tailor-made hemicellulose-based hydrogels reinforced with nanofibrillated cellulose. *Nordic Pulp & Paper Research Journal*, **30**(3), 373-384.
- Demir, A., Cevher, E. 2011. Biopolymers as Wound Healing Materials: Challenges and New Strategies. in: *Biomaterials Applications for Nanomedicine*, (Ed.) R. Pignatello, InTech. Croatia.
- Dong, S., Cho, H.J., Lee, Y.W., Roman, M. 2014. Synthesis and Cellular Uptake of Folic Acid-Conjugated Cellulose Nanocrystals for Cancer Targeting. *Biomacromolecules*, **15**(5), 1560-1567.
- Dugan, J.M., Collins, R.F., Gough, J.E., Eichhorn, S.J. 2013a. Oriented surfaces of adsorbed cellulose nanowhiskers promote skeletal muscle myogenesis. *Acta Biomaterialia*, **9**(1), 4707-4715.
- Dugan, J.M., Gough, J.E., Eichhorn, S.J. 2013b. Bacterial cellulose scaffolds and cellulose nanowhiskers for tissue engineering. *Nanomedicine*, **8**(2), 287-298.
- Dugan, J.M., Gough, J.E., Eichhorn, S.J. 2010. Directing the Morphology and Differentiation of Skeletal Muscle Cells Using Oriented Cellulose Nanowhiskers. *Biomacromolecules*, **11**(9), 2498-2504.
- Ebringerová, A., Hromádková, Z., Heinze, T. 2005. Hemicellulose. in: *Polysaccharides I-Structure, Characterization and Use*, (Ed.) T. Heinze, Vol. 186, Springer Berlin Heidelberg. New York, pp. 1-67.
- Eckardt, N.A. 2008. Role of xyloglucan in primary cell walls. *Plant Cell*, **20**(6), 1421-2.
- Eronen, P., Österberg, M., Heikkinen, S., Tenkanen, M., Laine, J. 2011. Interactions of structurally different hemicelluloses with nanofibrillar cellulose. *Carbohydrate Polymers*, **86**(3), 1281-1290.
- Fang, B., Wan, Y.-Z., Tang, T.-T., Gao, C., Dai, K.-R. 2009. Proliferation and Osteoblastic Differentiation of Human Bone Marrow Stromal Cells on Hydroxyapatite/Bacterial Cellulose Nanocomposite Scaffolds. *Tissue Engineering Part A*, **15**(5), 1091-1098.
- FitzPatrick, M., Champagne, P., Cunningham, M.F., Whitney, R.A. 2010. A biorefinery processing perspective: Treatment of lignocellulosic materials for the production of value-added products. *Bioresource Technology*, **101**(23), 8915-8922.
- Fowler, P.A., Hughes, J.M., Elias, R.M. 2006. Biocomposites: technology, environmental credentials and market forces. *Journal of the Science of Food and Agriculture*, **86**(12), 1781-1789.
- Frantz, C., Stewart, K.M., Weaver, V.M. 2010. The extracellular matrix at a glance. *Journal of Cell Science*,

123(24), 4195-4200.

- Fu, L., Zhang, J., Yang, G. 2013. Present status and applications of bacterial cellulose-based materials for skin tissue repair. *Carbohydrate Polymers*, **92**(2), 1432-1442.
- Fujisawa, S., Okita, Y., Fukuzumi, H., Saito, T., Isogai, A. 2011. Preparation and characterization of TEMPO-oxidized cellulose nanofibril films with free carboxyl groups. *Carbohydrate Polymers*, **84**(1), 579-583.
- Fukuzumi, H., Saito, T., Iwata, T., Kumamoto, Y., Isogai, A. 2009. Transparent and high gas barrier films of cellulose nanofibers prepared by TEMPO-mediated oxidation. *Biomacromolecules*, **10**(1), 162-5.
- Gandini, A., Lacerda, T.M., Carvalho, A.J., Trovatti, E. 2015. Progress of Polymers from Renewable Resources: Furans, Vegetable Oils, and Polysaccharides. *Chemical Reviews*, **116**(3), 1637-1669.
- George, J.T., Howard, G. 1963. Quantitative studies of the growth of mouse embryo cells in culture and their development into established lines. *The Journal of Cell Biology* **17**(2), 15.
- Goldschmid, O. 1954. Determination of Phenolic Hydroxyl Content of Lignin Preparations by Ultraviolet Spectrophotometry. *Analytical Chemistry*, **26**(9), 1421-1423.
- Habibi, Y. 2014. Key advances in the chemical modification of nanocelluloses. *Chemical Society Reviews*, **43**(5), 1519-1542.
- Hrebikova, H., Diaz, D., Mokry, J. 2015. Chemical decellularization: a promising approach for preparation of extracellular matrix. *Biomedical Papers*, **159**(1), 12-17.
- Hua, K., Carlsson, D.O., Ålander, E., Lindström, T., Strømme, M., Mihranyan, A., Ferraz, N. 2014. Translational study between structure and biological response of nanocellulose from wood and green algae. *RSC Advances*, **4**(6), 2892-2903.
- Itoh, S., Nakamura, S., Nakamura, M., Shinomiya, K., Yamashita, K. 2006. Enhanced bone ingrowth into hydroxyapatite with interconnected pores by Electrical Polarization. *Biomaterials*, **27**(32), 5572-9.
- Janmey, P.A., Miller, R.T. 2011. Mechanisms of mechanical signaling in development and disease. *Journal of Cell Science*, **124**(Pt 1), 9-18.
- Johansson, P., Brumer, H., 3rd, Baumann, M.J., Kallas, A.M., Henriksson, H., Denman, S.E., Teeri, T.T., Jones, T.A. 2004. Crystal structures of a poplar xyloglucan endotransglycosylase reveal details of transglycosylation acceptor binding. *Plant Cell*, **16**(4), 874-86.
- John, M., Thomas, S. 2008. Biofibres and biocomposites. *Carbohydrate Polymers*, **71**(3), 343-364.
- Jonoobi, M., Oladi, R., Davoudpour, Y., Oksman, K., Dufresne, A., Hamzeh, Y., Davoodi, R. 2015. Different preparation methods and properties of nanostructured cellulose from various natural resources and residues: a review. *Cellulose*, **22**(2), 935-969.
- Jorfi, M., Foster, E.J. 2015. Recent advances in nanocellulose for biomedical applications. *Journal of Applied Polymer Science*, **132**(14), 41719-41738.
- Joshi, M.K., Pant, H.R., Tiwari, A.P., Maharjan, B., Liao, N., Kim, H.J., Park, C.H., Kim, C.S. 2016. Three-dimensional cellulose sponge: Fabrication, characterization, biomimetic mineralization, and in vitro cell infiltration. *Carbohydrate Polymers*, **136**, 154-162.
- Junka, K., Filpponen, I., Lindström, T., Laine, J. 2013. Titrimetric methods for the determination of surface and total charge of functionalized nanofibrillated/microfibrillated cellulose (NFC/MFC). *Cellulose*, **20**(6), 2887-2895.
- Kamel, S. 2007. Nanotechnology and its applications in lignocellulosic composites, a mini review. *eXPRESS Polymer Letters*, **1**(9), 546-575.

- Kilpeläinen, P. 2012. Pressurized hot water extraction of acetylated xylan from birch sawdust. *Nordic Pulp and Paper Research Journal*, **27**(04), 680-688.
- Kilpeläinen, P., Kitunen, V., Pranovich, A., Ilvesniemi, H., Willfor, S. 2013. Pressurized Hot Water Flow-through Extraction of Birch Sawdust with Acetate pH Buffer. *Bioresources*, **8**(4), 5202-5218.
- Kilpeläinen, P.O., Hautala, S.S., Byman, O.O., Tanner, L.J., Korpinen, R.I., Lillandt, M.K.J., Pranovich, A.V., Kitunen, V.H., Willfor, S.M., Ilvesniemi, H.S. 2014. Pressurized hot water flow-through extraction system scale up from the laboratory to the pilot scale. *Green Chemistry*, **16**(6), 3186-3194.
- Klemm, D. 1998. *Comprehensive cellulose chemistry*. Wiley_VCH, Weinheim ; Chichester.
- Klemm, D., Heublein, B., Fink, H.P., Bohn, A. 2005. Cellulose: Fascinating biopolymer and sustainable raw material. *Angewandte Chemie-International Edition*, **44**(22), 3358-3393.
- Klemm, D., Kramer, F., Moritz, S., Lindstrom, T., Ankerfors, M., Gray, D., Dorris, A. 2011. Nanocelluloses: a new family of nature-based materials. *Angewandte Chemie International Edition*, **50**(24), 5438-66.
- Klemm, D., Schumann, D., Kramer, F., Heßler, N., Hornung, M., Schmauder, H.-P., Marsch, S. 2006. Nanocelluloses as Innovative Polymers in Research and Application. in: *Polysaccharides II*, (Ed.) D. Klemm, Vol. 205, Springer Berlin Heidelberg.
- Klemm, D., Schumann, D., Udhardt, U., Marsch, S. 2001. Bacterial synthesized cellulose — artificial blood vessels for microsurgery. *Progress in Polymer Science*, **26**(9), 1561-1603.
- Kolakovic, R., Laaksonen, T., Peltonen, L., Laukkanen, A., Hirvonen, J. 2012a. Spray-dried nanofibrillar cellulose microparticles for sustained drug release. *International Journal of Pharmaceutics*, **430**(1-2), 47-55.
- Kolakovic, R., Peltonen, L., Laukkanen, A., Hirvonen, J., Laaksonen, T. 2012b. Nanofibrillar cellulose films for controlled drug delivery. *European Journal of Pharmaceutics and Biopharmaceutics*, **82**(2), 308-315.
- Lanza, R.P., Langer, R.S., Vacanti, J. 2007. *Principles of tissue engineering*. 3rd ed. ed. Academic, London.
- Le Normand, M., Melida, H., Holmbom, B., Michaelsen, T.E., Inngjerdigen, M., Bulone, V., Paulsen, B.S., Ek, M. 2014. Hot-water extracts from the inner bark of Norway spruce with immunomodulating activities. *Carbohydrate Polymers*, **101**, 699-704.
- Leleux, P., Badier, J.-M., Rivnay, J., Bénar, C., Hervé, T., Chauvel, P., Malliaras, G.G. 2014. Conducting Polymer Electrodes for Electroencephalography. *Advanced Healthcare Materials*, **3**(4), 490-493.
- Leppänen, A.S., Xu, C.L., Liu, J., Wang, X.J., Pesonen, M., Willfor, S. 2013. Anionic Polysaccharides as Templates for the Synthesis of Conducting Polyaniline and as Structural Matrix for Conducting Biocomposites. *Macromolecular Rapid Communications*, **34**(13), 1056-1061.
- Lin, N., Dufresne, A. 2014. Nanocellulose in biomedicine: Current status and future prospect. *European Polymer Journal*, **59**, 302-325.
- Lin, S., Sangaj, N., Razafiarison, T., Zhang, C., Varghese, S. 2011a. Influence of physical properties of biomaterials on cellular behavior. *Pharmaceutical Research*, **28**(6), 1422-30.
- Lin, Y.K., Chen, K.H., Ou, K.L., Min, L. 2011b. Effects of different extracellular matrices and growth factor immobilization on biodegradability and biocompatibility of macroporous bacterial cellulose. *Journal of Bioactive and Compatible Polymers*, **26**(5), 508-518.
- Linder, A., Bergman, R., Bodin, A., Gatenholm, P. 2003. Mechanism of assembly of xylan onto cellulose surfaces. *Langmuir*, **19**(12), 5072-5077.
- Liu, J., Hu, H., Xu, J., Wen, Y. 2012. Optimizing enzymatic pretreatment of recycled fiber for improving

- its draining ability using response surface methodology. *BioResources*, **7**(2), 2121-2140.
- Lopez-Sanchez, P., Cersosimo, J., Wang, D., Flanagan, B., Stokes, J.R., Gidley, M.J. 2015. Poroelastic mechanical effects of hemicelluloses on cellulosic hydrogels under compression. *PLoS One*, **10**(3), e0122132.
- Luo, H., Xiong, G., Huang, Y., He, F., Wang, Y., Wan, Y. 2008. Preparation and characterization of a novel COL/BC composite for potential tissue engineering scaffolds. *Materials Chemistry and Physics*, **110**(2-3), 193-196.
- Malinen, M.M., Kanninen, L.K., Corlu, A., Isoniemi, H.M., Lou, Y.-R., Yliperttula, M.L., Urtti, A.O. 2014. Differentiation of liver progenitor cell line to functional organotypic cultures in 3D nanofibrillar cellulose and hyaluronan-gelatin hydrogels. *Biomaterials*, **35**(19), 5110-5121.
- Marchessault, R.H., Morehead, F.F., Walter, N.M. 1959. Liquid Crystal Systems from Fibrillar Polysaccharides. *Nature*, **184**(4686), 632-633.
- Markstedt, K., Mantas, A., Tournier, I., Martínez Ávila, H., Hägg, D., Gatenholm, P. 2015. 3D Bioprinting Human Chondrocytes with Nanocellulose–Alginate Bioink for Cartilage Tissue Engineering Applications. *Biomacromolecules*, **16**(5), 1489-1496.
- Mehling, T., Smirnova, I., Guenther, U., Neubert, R.H.H. 2009. Polysaccharide-based aerogels as drug carriers. *Journal of Non-Crystalline Solids*, **355**(50-51), 2472-2479.
- Mertaniemi, H., Escobedo-Lucea, C., Sanz-Garcia, A., Gandía, C., Mäkitie, A., Partanen, J., Ikkala, O., Yliperttula, M. 2016. Human stem cell decorated nanocellulose threads for biomedical applications. *Biomaterials*, **82**, 208-220.
- Michielsen, S. 2003. Specific Refractive Index Increments of Polymers in Dilute Solution. in: *The Wiley Database of Polymer Properties*, John Wiley & Sons, Inc.
- Miller, J. 2015. Production Summary of Cellulose Nanomaterials, Vol. Accessed 2016, <http://www.tappinano.org/whats-up/production-summary/>.
- Millon, L.E., Guhados, G., Wan, W. 2008. Anisotropic polyvinyl alcohol–Bacterial cellulose nanocomposite for biomedical applications. *Journal of Biomedical Materials Research Part B: Applied Biomaterials*, **86B**(2), 444-452.
- Moroni, L., de Wijn, J.R., van Blitterswijk, C.A. 2006. 3D fiber-deposited scaffolds for tissue engineering: influence of pores geometry and architecture on dynamic mechanical properties. *Biomaterials*, **27**(7), 974-85.
- Muiznieks, L.D., Keeley, F.W. 2013. Molecular assembly and mechanical properties of the extracellular matrix: A fibrous protein perspective. *Biochim Biophys Acta*, **1832**(7), 866-75.
- Müller, A., Ni, Z., Hessler, N., Wesarg, F., Müller, F.A., Kralisch, D., Fischer, D. 2013. The Biopolymer Bacterial Nanocellulose as Drug Delivery System: Investigation of Drug Loading and Release using the Model Protein Albumin. *Journal of Pharmaceutical Sciences*, **102**(2), 579-592.
- Muschler, G.F., Nakamoto, C., Griffith, L.G. 2004. Engineering Principles of Clinical Cell-Based Tissue Engineering. *The Journal of Bone & Joint Surgery*, **86**(7), 1541-1558.
- Nakayama, K.H., Hou, L., Huang, N.F. 2014. Role of Extracellular Matrix Signaling Cues in Modulating Cell Fate Commitment for Cardiovascular Tissue Engineering. *Advanced Healthcare Materials*, **3**(5), 628-641.
- Neves, S.C., Gomes, D.B., Sousa, A., Bidarra, S.J., Petrini, P., Moroni, L., Barrias, C.C., Granja, P.L. 2015. Biofunctionalized pectin hydrogels as 3D cellular microenvironments. *Journal of Materials Chemistry B*, **3**(10), 2096-2108.
- Nickerson, R.F., Habrle, J.A. 1947. Cellulose Intercrystalline Structure. *Industrial & Engineering Chemistry*,

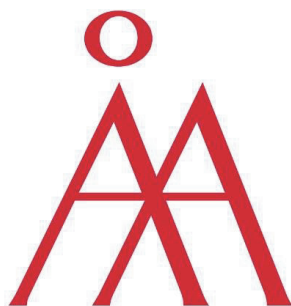
- 39(11), 1507-1512.
- Nishino, T., Matsuda, I., Hirao, K. 2004. All-Cellulose Composite. *Macromolecules*, **37**(20), 7683-7687.
- Nogi, M., Ifuku, S., Abe, K., Handa, K., Nakagaito, A.N., Yano, H. 2006. Fiber-content dependency of the optical transparency and thermal expansion of bacterial nanofiber reinforced composites. *Applied Physics Letters*, **88**(13), 133124.
- Nogi, M., Iwamoto, S., Nakagaito, A.N., Yano, H. 2009. Optically Transparent Nanofiber Paper. *Advanced Materials*, **21**(16), 1595-1598.
- Ohya, S., Nakayama, Y., Matsuda, T. 2001. Material design for an artificial extracellular matrix: Cell entrapment in poly (N-isopropylacrylamide) (PNIPAM)-grafted gelatin hydrogel. *Journal of Artificial Organs*, **4**(4), 308-314.
- Okay, O. 2010. General Properties of Hydrogels. in: *Hydrogel Sensors and Actuators*, (Eds.) G. Gerlach, K.-F. Arndt, Vol. 6, Springer Berlin Heidelberg, pp. 1-14.
- Okiyama, A., Motoki, M., Yamanaka, S. 1993. Bacterial cellulose IV. Application to processed foods. *Food Hydrocolloids*, **6**(6), 503-511.
- Oksman, K., Mathew, A.P., Sain, M. 2009. Novel bionanocomposites: processing, properties and potential applications. *Plastics, Rubber and Composites*, **38**(9-10), 396-405.
- Österberg, M., Vartiainen, J., Lucenius, J., Hippi, U., Seppala, J., Serimaa, R., Laine, J. 2013. A fast method to produce strong NFC films as a platform for barrier and functional materials. *ACS Applied Materials & Interfaces*, **5**(11), 4640-7.
- Pääkkö, M., Ankerfors, M., Kosonen, H., Nykänen, A., Ahola, S., Österberg, M., Ruokolainen, J., Laine, J., Larsson, P.T., Ikkala, O., Lindström, T. 2007. Enzymatic Hydrolysis Combined with Mechanical Shearing and High-Pressure Homogenization for Nanoscale Cellulose Fibrils and Strong Gels. *Biomacromolecules*, **8**(6), 1934-1941.
- Park, Y.B., Cosgrove, D.J. 2015. Xyloglucan and its Interactions with Other Components of the Growing Cell Wall. *Plant and Cell Physiology*, **56**(2), 180-194.
- Pei, A.H., Butchosa, N., Berglund, L.A., Zhou, Q. 2013. Surface quaternized cellulose nanofibrils with high water absorbency and adsorption capacity for anionic dyes. *Soft Matter*, **9**(6), 2047-2055.
- Pereira, M.M., Raposo, N.R.B., Brayner, R., Teixeira, E.M., Oliveira, V., Quintao, C.C.R., Camargo, L.S.A., Mattoso, L.H.C., Brandao, H.M. 2013. Cytotoxicity and expression of genes involved in the cellular stress response and apoptosis in mammalian fibroblast exposed to cotton cellulose nanofibers. *Nanotechnology*, **24**(7).
- Petersen, N., Gatenholm, P. 2011. Bacterial cellulose-based materials and medical devices: current state and perspectives. *Applied Microbiology and Biotechnology*, **91**(5), 1277-1286.
- Pfaltzgraff, L.A., Clark, J.H. 2014. Green chemistry, biorefineries and second generation strategies for re-use of waste: an overview. in: *Advances in Biorefineries*, (Ed.) K. Waldron, Woodhead Publishing, pp. 3-33.
- Plackett, D.V., Letchford, K., Jackson, J.K., Burt, H.M. 2014. A review of nanocellulose as a novel vehicle for drug delivery. *Nordic Pulp & Paper Research Journal*, **29**(1), 105-118.
- Plant, A.L., Bhadriraju, K., Spurlin, T.A., Elliott, J.T. 2009. Cell response to matrix mechanics: Focus on collagen. *Biochimica et Biophysica Acta (BBA) - Molecular Cell Research*, **1793**(5), 893-902.
- Popa, V. 2011. *Polysaccharides in Medicinal and Pharmaceutical Applications*. iSmithers, Shawbury, UK.
- Portal, O., Clark, W.A., Levinson, D.J. 2009. Microbial Cellulose Wound Dressing in the Treatment of Nonhealing Lower Extremity Ulcers. *Wounds-a Compendium of Clinical Research and Practice*, **21**(1), 1-3.

- Powell, L.C., Khan, S., Chinga-Carrasco, G., Wright, C.J., Hill, K.E., Thomas, D.W. 2016. An investigation of *Pseudomonas aeruginosa* biofilm growth on novel nanocellulose fibre dressings. *Carbohydrate Polymers*, **137**, 191-197.
- Prakobna, K., Kisonen, V., Xu, C., Berglund, L. 2015a. Strong reinforcing effects from galactoglucomannan hemicellulose on mechanical behavior of wet cellulose nanofiber gels. *Journal of Materials Science*, **50**(22), 7413-7423.
- Prakobna, K., Kisonen, V., Xu, C.L., Berglund, L.A. 2015b. Strong reinforcing effects from galactoglucomannan hemicellulose on mechanical behavior of wet cellulose nanofiber gels. *Journal of Materials Science*, **50**(22), 7413-7423.
- Ramanathan, G., Singaravelu, S., Raja, M.D., Nagiah, N., Padmapriya, P., Ruban, K., Kaveri, K., Natarajan, T.S., Sivagnanam, U.T., Perumal, P.T. 2016. Fabrication and characterization of a collagen coated electrospun poly(3-hydroxybutyric acid)-gelatin nanofibrous scaffold as a soft bio-mimetic material for skin tissue engineering applications. *RSC Advances*, **6**(10), 7914-7922.
- Ramanaviciene, A., Kausaite, A., Tautkus, S., Ramanavicius, A. 2007. Biocompatibility of polypyrrole particles: an in-vivo study in mice. *Journal of Pharmacy and Pharmacology*, **59**(2), 311-315.
- Revol, J.F., Godbout, L., Gray, D.G. 1998. Solid self-assembled films of cellulose with chiral nematic order and optically variable properties. *Journal of Pulp and Paper Science*, **24**(5), 146-149.
- Rimmer, S. 2011a. *Biomedical hydrogels : biochemistry, manufacture, and medical applications*. Woodhead Publishing, Cambridge, UK ; Philadelphia, PA.
- Rimmer, S.D. 2011b. *Biomedical hydrogels : biochemistry, manufacture and medical applications*. Woodhead Pub., Oxford.
- Saddiq, Z.A., Barbenel, J.C., Grant, M.H. 2009. The mechanical strength of collagen gels containing glycosaminoglycans and populated with fibroblasts. *Journal of Biomedical Materials Research Part A*, **89A**(3), 697-706.
- Saito, T., Isogai, A. 2004. TEMPO-mediated oxidation of native cellulose. The effect of oxidation conditions on chemical and crystal structures of the water-insoluble fractions. *Biomacromolecules*, **5**(5), 1983-9.
- Saito, T., Kimura, S., Nishiyama, Y., Isogai, A. 2007. Cellulose Nanofibers Prepared by TEMPO-Mediated Oxidation of Native Cellulose. *Biomacromolecules*, **8**(8), 2485-2491.
- Saito, T., Nishiyama, Y., Putaux, J.-L., Vignon, M., Isogai, A. 2006. Homogeneous Suspensions of Individualized Microfibrils from TEMPO-Catalyzed Oxidation of Native Cellulose. *Biomacromolecules*, **7**(6), 1687-1691.
- Saito, T., Uematsu, T., Kimura, S., Enomae, T., Isogai, A. 2011. Self-aligned integration of native cellulose nanofibrils towards producing diverse bulk materials. *Soft Matter*, **7**(19), 8804.
- Saska, S., Barud, H.S., Gaspar, A.M.M., Marchetto, R., Ribeiro, S.J.L., Messaddeq, Y. 2011. Bacterial Cellulose-Hydroxyapatite Nanocomposites for Bone Regeneration. *International Journal of Biomaterials*, **2011**, 1-8.
- Saska, S., Teixeira, L.N., Tambasco de Oliveira, P., Minarelli Gaspar, A.M., Lima Ribeiro, S.J., Messaddeq, Y., Marchetto, R. 2012. Bacterial cellulose-collagen nanocomposite for bone tissue engineering. *Journal of Materials Chemistry*, **22**(41), 22102.
- Sehaqui, H., Zhou, Q., Berglund, L.A. 2011. High-porosity aerogels of high specific surface area prepared from nanofibrillated cellulose (NFC). *Composites Science and Technology*, **71**(13), 1593-1599.
- Shi, Z., Phillips, G.O., Yang, G. 2013. Nanocellulose electroconductive composites. *Nanoscale*, **5**(8), 3194.
- Skotheim, T.A., Reynolds, J.R. 2007. *Handbook of conducting polymers. 3rd ed. / edited by Terje A.*

Skotheim and John R. Reynolds. ed. CRC, Boca Raton, Fla. ; London.

- Smits, F.M. 1958. Measurement of Sheet Resistivities with the Four-Point Probe. *Bell Systems Technical Journal* **37**(3), 711-718.
- Sorimachi, K., Watanabe, K., Yamazaki, S., Yasumura, Y. 1992. Inhibition of fibroblast growth by polyanions; effects of dextran sulfate and lignin derivatives. *Cell Biology International Reports*, **16**(1), 63-71.
- Spaic, M., Small, D., Cook, J., Wan, W. 2014. Characterization of anionic and cationic functionalized bacterial cellulose nanofibres for controlled release applications. *Cellulose*, **21**(3), 1529-1540.
- Stashak, T.S., Farstvedt, E., Othic, A. 2004. Update on wound dressings: Indications and best use. *Clinical Techniques in Equine Practice*, **3**(2), 148-163.
- Stella, J.A., D'Amore, A., Wagner, W.R., Sacks, M.S. 2010. On the biomechanical function of scaffolds for engineering load-bearing soft tissues. *Acta Biomaterialia*, **6**(7), 2365-81.
- Stevanic, J.S., Mikkonen, K.S., Xu, C.L., Tenkanen, M., Berglund, L., Salmen, L. 2014. Wood cell wall mimicking for composite films of spruce nanofibrillated cellulose with spruce galactoglucomannan and arabinoglucuronoxylan. *Journal of Materials Science*, **49**(14), 5043-5055.
- Sukul, M., Min, Y.-K., Lee, S.-Y., Lee, B.-T. 2015. Osteogenic potential of simvastatin loaded gelatin-nanofibrillar cellulose- β tricalcium phosphate hydrogel scaffold in critical-sized rat calvarial defect. *European Polymer Journal*, **73**, 308-323.
- Sun, R., Sun, X.F., Tomkinson, J. 2003. Hemicelluloses and Their Derivatives. in: *Hemicelluloses: Science and Technology*, (Eds.) P. Gatenholm, M. Tenkanen, Vol. 864, American Chemical Society. Washington, pp. 2-22.
- Syverud, K., Kirsebom, H., Hajizadeh, S., Chinga-Carrasco, G. 2011. Cross-linking cellulose nanofibrils for potential elastic cryo-structured gels. *Nanoscale Research Letters*, **6**, 626.
- Syverud, K., Pettersen, S., Draget, K., Chinga-Carrasco, G. 2015. Controlling the elastic modulus of cellulose nanofibril hydrogels—scaffolds with potential in tissue engineering. *Cellulose*, **22**(1), 473-481.
- Torres-Rendon, J.G., Femmer, T., De Laporte, L., Tigges, T., Rahimi, K., Gremse, F., Zafarnia, S., Lederle, W., Ifuku, S., Wessling, M., Hardy, J.G., Walther, A. 2015. Bioactive Gyroid Scaffolds Formed by Sacrificial Templating of Nanocellulose and Nanochitin Hydrogels as Instructive Platforms for Biomimetic Tissue Engineering. *Advanced Materials*, **27**(19), 2989-2995.
- Turbak, A.F., Snyder, F.W., Sandberg, K.R. 1983. Microfibrillated cellulose, Vol. Patent 4374702 A. U.S.
- Utah, U.o. 2016. Cell Size and Scale.
- Valo, H., Arola, S., Laaksonen, P., Torkkeli, M., Peltonen, L., Linder, M.B., Serimaa, R., Kuga, S., Hirvonen, J., Laaksonen, T. 2013. Drug release from nanoparticles embedded in four different nanofibrillar cellulose aerogels. *European Journal of Pharmaceutical Sciences*, **50**(1), 69-77.
- Vandamme, E.J., De Baets, S., Vanbaelen, A., Joris, K., De Wulf, P. 1998. Improved production of bacterial cellulose and its application potential. *Polymer Degradation and Stability*, **59**(1-3), 93-99.
- Wågberg, L., Decher, G., Norgren, M., Lindstrom, T., Ankerfors, M., Axnas, K. 2008. The build-up of polyelectrolyte multilayers of microfibrillated cellulose and cationic polyelectrolytes. *Langmuir*, **24**(3), 784-795.
- Wan, W.K., Hutter, J.L., Milton, L., Guhados, G. 2006. Bacterial Cellulose and Its Nanocomposites for Biomedical Applications. in: *Cellulose Nanocomposites*, (Eds.) K. Oksman, M. Sain, Vol. 938, American Chemical Society. Washington, pp. 221-241.

- Wan, Y., Gao, C., Han, M., Liang, H., Ren, K., Wang, Y., Luo, H. 2011. Preparation and characterization of bacterial cellulose/heparin hybrid nanofiber for potential vascular tissue engineering scaffolds. *Polymers for Advanced Technologies*, **22**(12), 2643-2648.
- Wang, J., Gao, C., Zhang, Y., Wan, Y. 2010. Preparation and in vitro characterization of BC/PVA hydrogel composite for its potential use as artificial cornea biomaterial. *Materials Science and Engineering: C*, **30**(1), 214-218.
- Wells, R.G. 2008. The role of matrix stiffness in regulating cell behavior. *Hepatology*, **47**(4), 1394-1400.
- Wells, R.G. 2013. Tissue mechanics and fibrosis. *Biochimica et Biophysica Acta*, **1832**(7), 884-90.
- Willför, S., Nisula, L., Hemming, J., Reunanen, M., Holmbom, B. 2004. Bioactive phenolic substances in industrially important tree species. Part 1: Knots and stemwood of different spruce species. *Holzforschung*, **58**(4).
- Willför, S., Rehn, P., Sundberg, A., Sundberg, K., Holmbom, B. 2003. Recovery of water-soluble acetylgalactoglucomannans from mechanical pulp of spruce. *TAPPI JOURNAL*, **2**(11), 27-32.
- Winter, G.D. 1962. Formation of the scab and the rate of epithelization of superficial wounds in the skin of the young domestic pig. *Nature*, **193**, 293-4.
- Xu, C., Leppanen, A.S., Eklund, P., Holmlund, P., Sjöholm, R., Sundberg, K., Willfor, S. 2010. Acetylation and characterization of spruce (*Picea abies*) galactoglucomannans. *Carbohydrate Reserch*, **345**(6), 810-6.
- Xu, C., Spadiut, O., Araújo, A.C., Nakhai, A., Brumer, H. 2012. Chemo-enzymatic Assembly of Clickable Cellulose Surfaces via Multivalent Polysaccharides. *ChemSusChem*, **5**(4), 661-665.
- Yamanaka, S., Watanabe, K., Kitamura, N., Iguchi, M., Mitsuhashi, S., Nishi, Y., Uryu, M. 1989. The structure and mechanical properties of sheets prepared from bacterial cellulose. *Journal of Materials Science*, **24**(9), 3141-3145.
- Yang, T., Malkoch, M., Hult, A. 2013. Sequential interpenetrating poly(ethylene glycol) hydrogels prepared by UV-initiated thiol-ene coupling chemistry. *Journal of Polymer Science Part A: Polymer Chemistry*, **51**(2), 363-371.
- Yano, H., Sugiyama, J., Nakagaito, A.N., Nogi, M., Matsuura, T., Hikita, M., Handa, K. 2005. Optically Transparent Composites Reinforced with Networks of Bacterial Nanofibers. *Advanced Materials*, **17**(2), 153-155.
- Yoshinaga, F., Tonouchi, N., Watanabe, K. 2014. Research Progress in Production of Bacterial Cellulose by Aeration and Agitation Culture and Its Application as a New Industrial Material. *Bioscience, Biotechnology and Biochemistry*, **61**(2), 219-224.



Åbo Akademi



Graduate School in Chemical Engineering



Johan Gadolin
PROCESS CHEMISTRY CENTRE

ISBN 978-952-12-3424-8

Painosalama Oy – Turku, Finland 2016